AWARD NUMBER: W81XWH-19-1-0008

TITLE: Targeting Ovarian Cancer Stem Cells Interactions with the Niche

PRINCIPAL INVESTIGATOR: Salvatore Condello, PhD

CONTRACTING ORGANIZATION: Indiana University School of Medicine
340 West 10th Street
Fairbanks Hall, Suite 6200
Indianapolis, IN 46202-3082

REPORT DATE: August 2021

TYPE OF REPORT: Annual

PREPARED FOR: U.S. Army Medical Research and Development Command
Fort Detrick, Maryland 21702-5012

REPORT DOCUMENTATION PAGE

Form Approved
OMB No. 0704-0188

1. REPORT DATE	2. REPORT TYPE	3. DATES COVERED
August 2021	Annual	August 1, 2020–July 31,2021

4. TITLE AND SUBTITLE
Targeting Ovarian Cancer Stem Cells Interactions with the Niche

5a. CONTRACT NUMBER

5b. GRANT NUMBER
W81XWH-19-1-0008

5c. PROGRAM ELEMENT NUMBER

6. AUTHOR(S)
Salvatore Condello, PhD

E-Mail: salvcond@iu.edu

5d. PROJECT NUMBER

5e. TASK NUMBER

5f. WORK UNIT NUMBER

7. PERFORMING ORGANIZATION NAME(S) AND ADDRESS(ES)
Indiana University School of Medicine
340 West 10th Street
Fairbanks Hall, Suite 6200
Indianapolis, In 46202

8. PERFORMING ORGANIZATION REPORT NUMBER

9. SPONSORING / MONITORING AGENCY NAME(S) AND ADDRESS(ES)
U.S. Army Medical Research and Development Command
Fort Detrick, Maryland 21702-5012

10. SPONSOR/MONITOR'S ACRONYM(S)

11. SPONSOR/MONITOR'S REPORT NUMBER(S)

12. DISTRIBUTION / AVAILABILITY STATEMENT
Approved for Public Release; Distribution Unlimited

13. SUPPLEMENTARY NOTES

14. ABSTRACT
Ovarian cancer (OC) recurrence and spread have been linked to a small population of cancer stem cells (CSC), which are resistant to traditional chemotherapy. Tissue transglutaminase (TG2), an enzyme found to be active in ovarian tumors, protects CSCs and stimulates their growth. We found that this enzyme is enriched at the membrane of OC cells forming a complex with several receptors, such as integrins and the Wnt receptors Frizzled 1, 7 and co-receptor LRP6. This interaction stimulates survival pathways linked with the integrin linked kinase (ILK) activation and CD166 expression in OC cells and maintains the CSC phenotype. We defined the amino acids residues involved in the TG2/Fzd7 interaction and we are using this discovery to design a new treatment for OC by generating an antibody that could disrupt the complex. Our research has several important implications. First, we defined TG2 as novel Wnt pathway co-receptor. Second, the Wnt receptors in a complex with TG2 activate Wnt signals promoting the expression of several stemness-related genes (ALDH1A1, Sox2, and Nanog) and the novel proposed CSC marker CD166 involved in OCSCs' proliferation as spheres. Third, we expanded our research identifying a new functional link between the TG2 regulated cell adhesion to the matrix, integrin linked kinase (ILK) phosphorylation and canonical Wnt signaling activation, proposing ILK as a central node of two combinatorial signals. These results point to TG2/Wnt receptors as potential new therapeutic CSC targets.

15. SUBJECT TERMS
Ovarian cancer, tumors, ovarian cancer stem cells, tissue transglutaminase, frizzled 1, frizzled 7, LRP6, CD166, ILK, phospho ILK, synthetic peptides, recombinant proteins, expression plasmids, therapeutic target

16. SECURITY CLASSIFICATION OF:			17. LIMITATION OF ABSTRACT	18. NUMBER OF PAGES	19a. NAME OF RESPONSIBLE PERSON
a. REPORT	b. ABSTRACT	c. THIS PAGE			USAMRMC
Unclassified	Unclassified	Unclassified	Unclassified	27	19b. TELEPHONE NUMBER *(include area code)*

TABLE OF CONTENTS

Page

1. Introduction

Epithelial ovarian cancer (EOC) is the most lethal of all gynecologic malignancies, with the majority of cases being diagnosed at an advanced stage. Current standard treatment of OC, in both early and advanced stages, consists of complete cytoreductive surgery followed by chemotherapy, usually based on platinum/taxane combination. The initial response rate is high (70%-80%); but the majority of patients with advanced disease relapse within the first five years after diagnosis resulting in a cycle of repeated surgeries and additional rounds of chemotherapy.

Recurrent ovarian cancer is not curable, due to the development of chemoresistance. Both recurrence and spread have been linked to a small population of OC cells called ovarian cancer stem cells (OCSCs), which are resistant to traditional chemotherapy. The accumulation of ascites in the abdomen provides a favorable environment, enriched in growth factors and proteins that protect the quiescent OCSCs during chemotherapy and promote their growth. To date, treatment strategies designed to eliminate the genesis of the OCSCs still remain a significant challenge. One main obstacle toward a successful treatment option for OC remains the molecular identification of these tumorigenic cells.

Recent work by our group and others demonstrated that the multifunctional protein tissue transglutaminase (TG2), with enzymatic and scaffold functions, is an important molecule secreted in the tumor microenvironment (TME) where it modulates oncogenic signaling by interacting with extracellular matrix (ECM) components, such as fibronectin (FN) and integrins. Its aberrant expression was correlated with OC progression and with the tumorigenic OCSC phenotype. Our data indicate that the formation of the TG2/FN/β1 integrin ternary complex at the cell membrane activates the oncogenic Wnt/β-catenin pathway by specifically engaging the Wnt receptor Frizzled7 (Fzd7), leading to the canonical β-catenin pathway activation and OCSC proliferation as spheroids. The Aim 2 of this proposed research plan is to define the mechanism by which TG2/Fzd complexes regulate β-catenin transcriptional activity in OC cells and tumors promoting stemness.

Our findings during the first two years of funded period linked the discovery of the mesenchymal stem cell marker CD166 as possible gene regulated by the TG2/Fzd7 axis, supporting the role of TG2/Fzd7 interaction as OCSC regulators. We also expanded our research identifying a new functional link between the TG2 regulated cell adhesion to the matrix, integrin linked kinase (ILK) phosphorylation and canonical Wnt signaling activation, proposing ILK as a central node of two combinatorial signals and as a possible therapeutic target. In addition, we defined the key amino acids residues involved in the TG2/Fzd7 interaction. This discovery will allow us to synthesize a KLH-conjugated peptide that will be used to produce an antibody raised against the TG2/Fzd7 interacting amino acids. Finally, we discovered the Wnt receptor Frizzled 1 (FZD1) and the co-receptor LRP6 as two new possible interacting partners for TG2.

In conclusion, the preliminary data obtained during the funded period provided strong evidence supporting a key function of TG2/Wnt receptors complexes in OCSCs. By demonstrating that TG2 directly binds the Fzd1, 7 receptors and LRP6 co-receptor, we identified a novel function of TG2 and a new mechanism promoting CSCs' proliferation and tumorigenicity. These results point to the newly discovered co-receptor complexes TG2/Fzd1, 7, and LRP6 as potential new therapeutic CSC targets.

2. Keywords

Ovarian cancer, tumors, ovarian cancer stem cells, tissue transglutaminase, frizzled 1, frizzled 7, ILK, phospho ILK, LRP6, CD166, synthetic peptides, recombinant proteins, expression plasmids, therapeutic target.

3. Accomplishments

The annual accomplishments are summarized in the following Annual Research Progress

A) Annual Research progress

What were the major goals of the project?

Major Goals of the project.

Specific Aim 1: Biochemical definition of TG2/Fzd receptors interaction leading to β-catenin activation in OC. Months 1-12

Major Task 1: Define the structural characteristics of the TG2/Fzd7 interaction in ovarian cancer stem cells. Completed 100%

Subtask 1: Build a robust homology model of the human Fzd7 and other Fzd receptors and LRP co-receptors. Use this model to identify novel putative protein-protein interactions between TG2 and Fzd7 or other Wnt receptors. Months 3-8. Completed 50%

Subtask 2: Co-IP of full length recombinant Fzd7 and other Fzd and LRP proteins with full-length and recombinant TG2 fragments harboring truncations or mutations. Months 3-8. Completed 50%

Subtask 3: Transfection ovarian cancer cell lines with plasmids encoding Myc-DDK-tagged Human Fzds, Flag-tagged LRPs and Histidine (His)-tagged TG2 mutants and wild-type. Months 6-12. Completed 40%

Subtask 4: Tumor biopsies collection, HGSOC spheroids and PDX organoids generation and tissue slides preparation. Months 1-12. Completed 70%

Subtask 5: Immuno-staining for TG2/Fzds and TG2/LRPs complexes by PLA on human ovarian tumors, human fallopian tube epithelium, HGSOC spheroids, and organoids from PDX. Months 1-12. Completed 30%

Milestone(s) Achieved:
1) Define the molecular interaction between TG2/Fzd7 and other Fzd receptors and co-receptors. Completed 50%
2) Test this novel co-receptor complex in the ability to activate the Wnt pathway in OC cells. Completed 50%

Major Task 3: Define the mechanism by which TG2/Fzd regulates beta-catenin activity in OC and stemness. Months 12-48.

Milestone(s) Achieved: 1) Analyze TG2/Fzd complexes in promoting the gene signature correlated with CSC phenotype; 2) Mapping TG2/Fzds expression in correlation with Wnt ligands, receptors, downstream signaling and target molecules in the heterogenous tumor populations; 3) Complete manuscript 1 preparation and submission. Complete 40%

Major Goals of the project.

Specific Aim3: Develop novel strategies to target Wnt/β-catenin activity in OC. Months 24-48.

Major Task 5: Generate function-blocking antibodies that target TG2/Fzd7 complex in CSCs. Months 24-36.
Subtask 1: Synthesizing, purifying, and characterizing custom peptides based on residues of Fzd7 and other frizzled receptors interacting with TG2. Months 24-36. Complete 25%

Milestone(s) Achieved: Definition and synthesis of custom peptides directed against TG2/Fzd7 complex. Provide newly purified mAbs directed against TG2/Fzd7 co-receptor complex and validate their ability to disrupt CSC survival and proliferation by blocking beta-catenin signaling. Complete 50%

Obtain IRB approval for the project- Obtained on May 14, 2019- Complete*
*Note: The Indiana University Human Research Protection Program has determined that the above-referenced project does not require IRB review for the following reason:
. Project does not involve human subjects as defined in 45 CFR 46.102(f)
. Study meets the criteria for approval defined by the HRPP Policy on IRB Review Process

Obtain ORP HRPO approval for the project- Obtained on August 05, 2019- Complete*
*Note: SUBJECT: HRPO Concurrence with the Determination of Research Not Involving Human Subjects for the Protocol, "Targeting Ovarian Cancer Stem Cells Interactions with the Niche," Submitted by Salvatore Condello, PhD, Indiana University School of Medicine, Indianapolis, Indiana, Proposal Log Number OC180384, Award Number W81XWH-19-1-0008, HRPO Log Number E01114.1a
As required by DOD Instruction 3216.02, encl 3, paragraph 4.c(1), the ORP HRPO concurs with the IU Human Research Program determination of research not involving human subjects. The project may proceed with no further requirement for review by the HRPO. The HRPO protocol file will be closed.

Obtain local IBC approval for the project- Obtained on June 03, 2019- Complete

Obtain ACURO approval for the project- Obtained on June 04, 2020- Complete

Major Task 2: Interrogate the mechanism through which this novel co-receptor complex activates the Wnt pathway in OCSCs. Months 12-24.

Subtask 1: Tumor biopsies collection, HGSOC spheroids and PDX organoids generation and tissue slides preparation. Months 12-24. Complete 70%

Subtask 2: Isolation of primary cells from tumor biopsies. Months 12-24. Complete 70%

Subtask 3: Co-IP and IF in HGSOC spheroid (OVCAR-3-4-5-8, HEY, COV362, SKOV3 OC cell lines and human tumors or ascites) to detect TG2 complexes. Months 12-24. Complete 50%

Subtask 4: IHC on tumor sections to detect localization of TG2 with frizzled receptors and LRP co-receptors. PLA on tumor sections to detect spatial localization and interaction of TG2 with frizzled receptors and LRP co-receptors. Months 12-24. Complete 50%

Subtask 5: Transfection of ovarian cancer cell lines with plasmids encoding Myc-DDK-tagged Human Fzd7 or other Wnt receptors and coreceptors and Histidine (His)-tagged TG2 mutants and wild-type. Months 12-24. Complete 50%

Subtask 6: Sphere formation assay, Topflash TCF/LEF1 reporter assay, RNA-DNA extraction from cells, qRT-PCR for beta-catenin target genes, and active beta-catenin cellular localization. Months 12-24. Complete 50%

Milestone(s) Achieved: 1) Define the mechanism through which this novel co-receptor complex activates the Wnt pathway in OCSCs; 2) Present data at DOD meeting; 3) Start preparation of manuscripts 1 and 2.

Specific Aim 2
Major Task 3: Define the mechanism by which TG2/Fzd regulates beta-catenin activity in OC and stemness. Months 12-48. Complete 50%

Specific Aim 3
Major Task 4: Test TG2/Fzd complexes in promoting the OC chemo-resistant phenotype.
Months 24-36. Complete 30%

What was accomplished under these goals?

One of the goals of the proposed research was to define the mechanism by which TG2/Fzds complexes regulate β-catenin transcriptional activity in OC cells and tumors promoting stemness (Aim 2). During the funded period our major accomplishment was to define two main targets regulated by TG2 interaction with elements of the Wnt pathway, which are summarized in two ongoing projects:
Project 1: CD166 as novel therapeutic target to overcome platinum resistance in ovarian cancer
Project 2: Tissue transglutaminase mediated integrin-linked kinase activation is a key regulator of Wnt/β-catenin signaling in ovarian cancer

Project 1:
CD166 as novel therapeutic target to overcome platinum resistance in ovarian cancer

1) CD166 *m*RNA expression is enriched in OC cells growing as 3D compared with 2D cultures: Primary OC cells derived from three different patient's malignant ascites were profiled using specific PCR arrays (RT² Profiler PCR Array, Qiagen) for genes relevant to CSCs. The most up-regulated genes were correlated with the Wnt/β-catenin pathway (Fzd7, Myc, and Wnt1) and the CSC markers (ALCAM, ALDH1A1, CD24, CD44, and KIT) (Table 1). One of the genes significantly upregulated in the three primary OC cells grown as spheroids compared to monolayers was the activated leukocyte cell adhesion molecule (ALCAM), also known as CD166 (cluster of differentiation 166). This protein is one of the cell adhesion molecules involved in tumor progression and its modulation impacts the crosstalk between cell-cell and cell-matrix adhesion, leading to impaired ability of tumor cells to

Table 1: CSC related genes preferentially up-regulated in primary OC spheroids compared to monolayers (≥2.0-fold change)

Symbol	Gene Description	Gene Name	Fold change
NM_001627	ALCAM	Activated leukocyte cell adhesion molecule	6.1
NM_000689	ALDH1A1	Aldehyde dehydrogenase 1 family, member A1	4.1
NM_005430	Wnt1	Wingless-type MMTV integration site family, member 1	2.1
NM_013230	CD24	CD24 molecule	2.4
NM_000610	CD44	CD44 molecule (Indian blood group)	2.4
NM_003507	Fzd7	Frizzled family receptor 7	5.4
NM_000222	KIT	V-kit Hardy-Zuckerman 4 feline sarcoma viral oncogene homolog	2.6
NM_002467	MYC	V-myc myelocytomatosis viral oncogene homolog (avian)	2.4

Table 1: CSC-related genes enriched in OC spheroids compared to monolayers. List of genes preferentially up-regulated in primary OC cells grown as spheroids compared to monolayers were quantified by RT² Profiler PCR array (≥2.0-fold change).

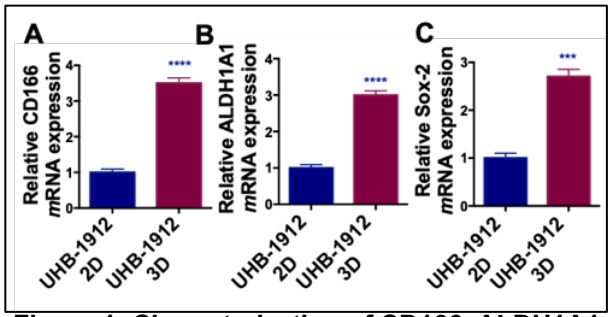

Figure 1: Characterization of CD166, ALDH1A1, and Sox-2 expression in OC primary cells. Real-time PCR of CD166, ALDH1A1, Sox-2 *m*RNA levels in human ovarian spheroids (3D) compared to monolayers (2D). (N=3; ***P<0.001; ****P<0.0001).

metastasize. Despite a functional role in the tumorigenic CSC phenotype and overexpression in metastatic compared with normal tissues, how CD166 is regulated during OC progression remains poorly understood. Our preliminary data functionally linking CD166 to the tumorigenic CSC phenotype and its overexpression in metastatic tissues provide a strong rationale to investigate this molecule as a potential new therapeutic target in OC.

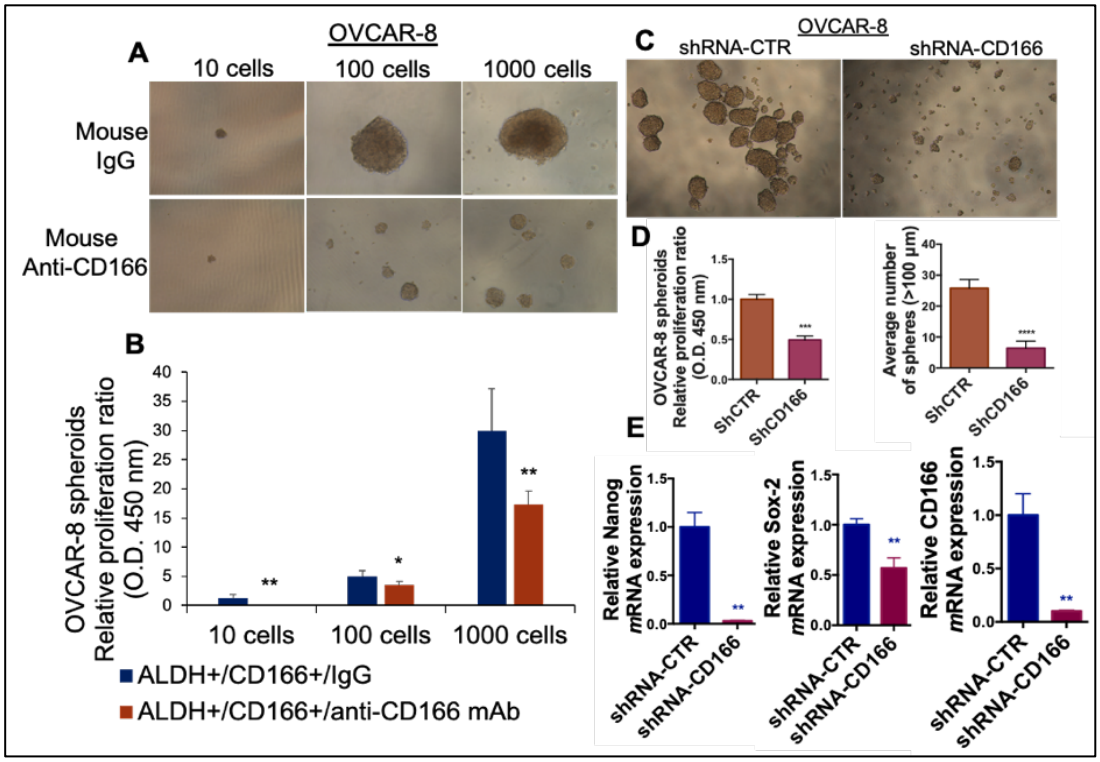

Figure 2: CD166 targeting in OC immortalized cells. A. Phase contrast microscopy of serial dilutions (10, 100, 1000) of FACS-sorted ALDH$^+$/CD166$^+$ OVCAR-8 cells grown as spheroids and treated for 21 days with mouse IgG control (10 µg/ml) or anti-CD166 mAb (10 µg/ml). **B.** CCK-8 assay quantifies proliferation of spheroids from OVCAR-8 cells with inhibitory anti-CD166 mAb (N=3; *P<0.05; **P<0.01). **C.** Phase contrast microscopy of spheroids formation in OVCAR-8 cells stably transduced with control- and CD166-targeting shRNA. **D.** CCK-8 quantification (left panel) and average number of spheroids count (>100 µm) (right panel) of OVCAR-8 cells transduced with shRNA control vs. shRNA-CD166 and grown as spheroids (N=3; ***P<0.001; ****P<0.0001). **E.** Real-time PCR of Nanog, Sox-2, and CD166 *m*RNA in OVCAR-8 shRNA-CD166 spheroids compared to shRNA-control (N=3; **P<0.01).

In previous studies, we and others have demonstrated that OC cells growing as spheroids under non-differentiating conditions are enriched in CSCs compared with cells growing as monolayers. In OC spheroids vs monolayers, CD166 expression levels were significantly upregulated across several OC cell lines (HEY-A8, OVCAR-5-8, COV362) and primary OC cells derived from malignant ascites (Fig. 1A). Expression of stemness-associated genes (ALDH1A1 and Sox-2) were increased in human primary OC spheroids vs. monolayers (Fig. 1B, C), consistent with OCSC phenotype.

2) CD166 functional inhibition disrupts spheroid formation and blocks OCSCs: The role of CD166 in cell adhesion and capacity to form homodimers across adjacent cell membranes has been reported suggests a function for this molecule within the tumor niche. We used an inhibitory monoclonal antibody (mAb) and gene silencing to block CD166 and examine its role in OCSC. Serial dilution (10, 100, 1000) of FACS-sorted ALDH$^+$/CD166$^+$ in four OC cell lines (HEY-A8, OVCAR-5-8, COV362) treated with anti-CD166 mAb (clone # AZN-L50) decreased spheroid proliferation (Fig. 2A, B). Additionally, shRNA-mediated CD166 knock down (KD) prevented spheroids formation in these four OC cell lines as shown by microscopic examination (Figure 2C), CCK-8 colorimetric proliferation assay, and spheres count (diameter greater than 100 µm; (Fig. 2D, left

and right panels). Real-time PCR confirmed CD166 KD and corresponding downregulation of Nanog and Sox-2 (Fig. 2E). We and others have identified ALDH1A1, a cancer stem cell marker as being overexpressed in OC spheroids and directly connected to key elements of the oncogenic β-catenin pathway. OVCAR-8 cells lack in

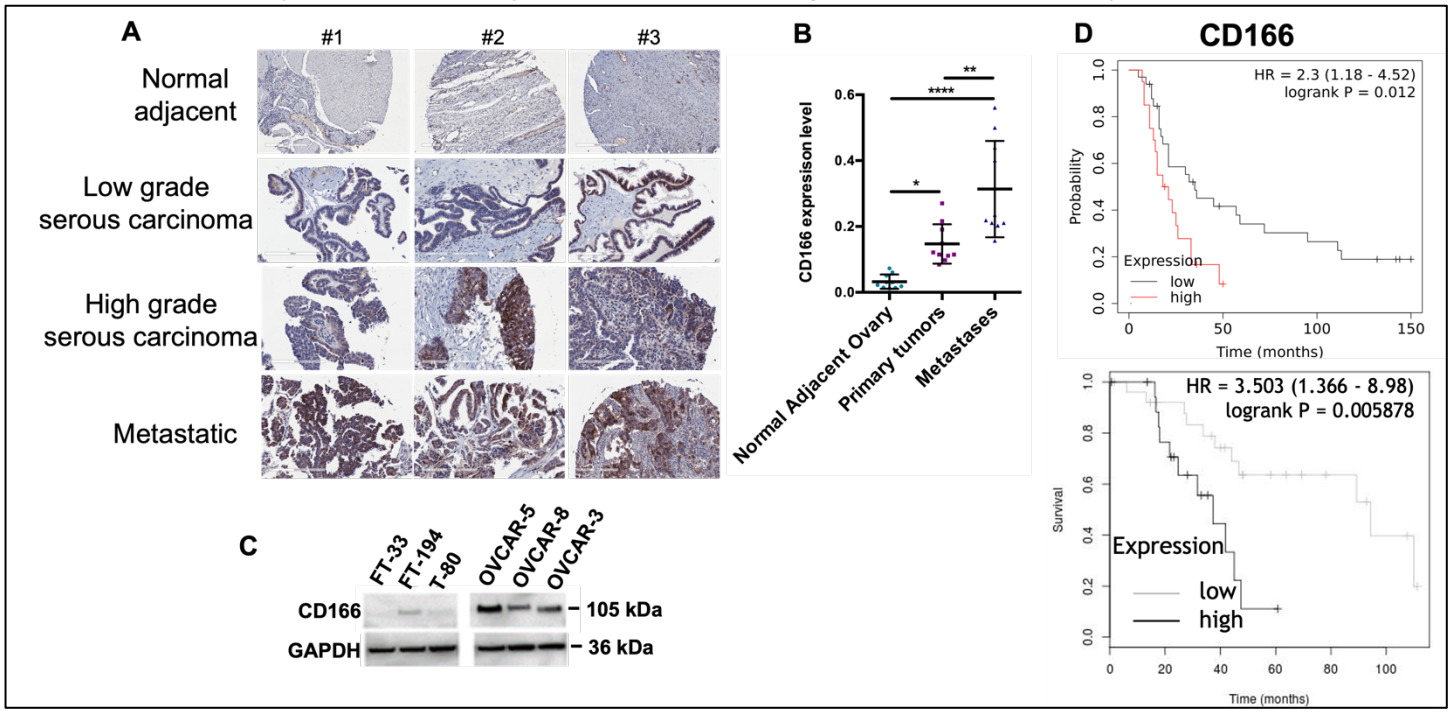

Figure 3: Increased CD166 expression confers poor prognosis in patients with HGSOC. A. Representative core images for low, medium, and high CD166 levels in low and HGSOC tumors (n = 88 total), metastasis (n = 10), adjacent normal ovaries (n = 10) in TMA of patients with HGSOC, scale bar 400 µm. **B.** Quantification of CD166 expression (H-score) by digital scanning of the TMA. **C.** Relative CD166 protein levels in HGSOC OVCAR3/5/8, normal ovarian epithelium (T-80) and fallopian tube (FT-33/194) cells. **D.** Overall survival curves generated using the Kaplan–Meier plotter (upper panel) and OvMark (lower panel) for tumors expressing high levels of CD166 versus those expressing low levels of CD166 (P = 0.012 and P = 0.005, respectively).

ALDH1A1 expression. In our data, we have demonstrated that OVCAR-8 cells FACS-sorted for CD166 alone were enriched in CSC markers (Nanog and Sox2) and were able to form compact spheroids (Fig. 2). The evidence supports the hypothesis of CD166 as independent OCSC marker. We will pursue our studies in OVCAR-8 cells to validate CD166 as new OCSC marker.

4) CD166 as independent marker of survival. CD166 upregulation has been correlated to patient outcome for several cancers. A comparison of normal adjacent ovarian epithelium, localized and metastatic ovarian cancer tissues on in-house multitissue array (TMA) revealed that CD166 expression was low to undetectable in normal ovary and increased in high-grade serous specimens and metastatic disease, coinciding with an advanced promigratory phenotype (n= 88, * P<0.05, ** P<0.01, **** P<0.0001, Fig. 3A-B). In agreement with these data, western blot analysis revealed that CD166 was expressed in HGSOC (OVCAR-3/5/8) cell lines and that non-tumorigenic cells, including human ovarian surface epithelial (HOSE) T80, and human fallopian tube FT33 and FT194 expressed low or undetectable CD166 (Fig. 3C). Survival analysis using the Kaplan– Meier plotter and an in-house cohort of Molecular Therapeutics for Cancer, Ireland (MTCI) using OVMARK revealed a significant association of high CD166 levels with poor overall survival of patients with HGSOC (Fig. 3D; P=0.012 and P=0.005, respectively). These data support the significance of CD166 at the interface with the ECM in human ovarian tumors affecting clinical outcomes.

CD166 expression is correlated with therapy resistance

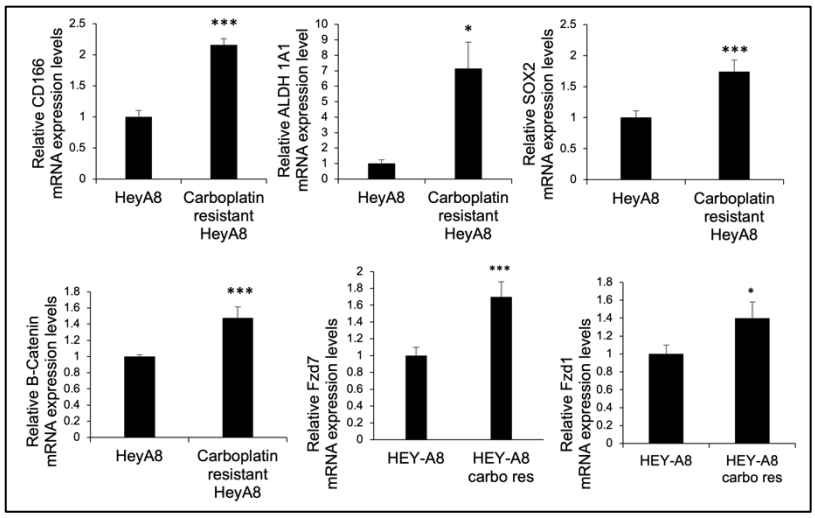

Figure 4. CD166 expression is increased in chemoresistant OC cells. Real-time PCR for CD166, ALDH1A1, Sox-2, β-catenin, Fzd1 and 7 in HEY-A8 chemo sensitive vs chemoresistant cells grown as spheroids (N=4; *P<0.05; ***P<0.001).

Therapy resistance is a major problem when treating patients with OC as cancer cells develop mechanisms that counteract the effect of therapeutic compounds, leading to fit and more aggressive clones that contribute to poor prognosis. CSCs represent the major source of therapy resistance. Our analysis demonstrated an increase in CD166 expression levels in chemo resistant OC cell lines when compared to the chemo sensitive counterpart (OVCAR-8 showed). The increase in CD166 level was correlated with a correspondent increase in other CSC markers, such as ALDH1A1 and Sox-2 and elements of the Wnt pathway, including β-catenin and the Frizzled receptors Fzd1 and 7 (Fig. 4; n=3; *P<0.05; **P<0.01; ***P<0.001).

To understand whether CD166 has a functional role in chemoresistance, we treated OC cells grown as spheroids with the AZN-L50 mAb that specifically blocks the CD166-mediated homotypic interactions. AZN-L50 treatment blocked spheroids and colony formation at the same extent of carboplatin when compared to

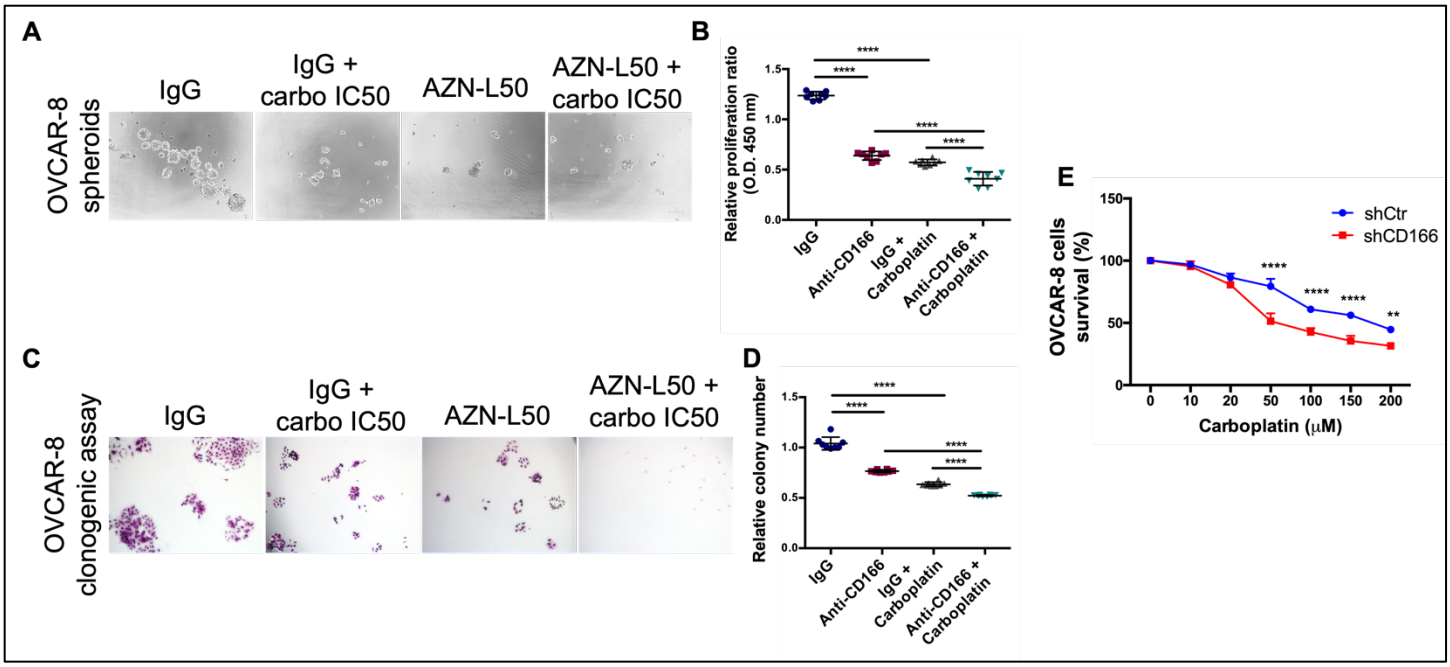

Figure 5: CD166 targeting in OC immortalized cells. A. Phase contrast microscopy of OVCAR-8 cells grown as spheroids and treated for 7 days with mouse IgG control (10 μg/ml), anti-CD166 mAb (10 μg/ml), carboplatin (IC50) and combination. **B.** CCK-8 assay quantifies proliferation of spheroids from OVCAR-8 cells with inhibitory anti- CD166 mAb, carboplatin (IC50), and combination (N=8; ****P<0.0001). **C.** Phase contrast microscopy of colony formation in OVCAR-8 cells treated for 7 days with mouse IgG control (10 μg/ml), anti-CD166 mAb (10 μg/ml), carboplatin (IC50) and combination. **D.** Quantification of crystal violet-stained cell colonies (N=8; ****P<0.0001). **E.** Effects of carboplatin (10 μM – 200 μM) in OVCAR-8 cells stably transduced with control- and CD166-targeting shRNA and grown as spheroids. Dose–response curves representing sphere numbers and the percentage of surviving cells were plotted using GraphPad Prism against the concentrations of carboplatin used during a 72 h treatment period (n=8; **P<0.01, ****P<0.0001.

A

CSC-related genes preferentially down-regulated in OC spheroids by 4G3 treatment compared to IgG control (≥2.0-fold change)

Symbol	Gene Description	Gene Name	Fold change
NM_001627	ALCAM	Activated leukocyte cell adhesion molecule	-54.4
NM_000689	ALDH1A1	Aldehyde dehydrogenase 1 family, member A1	-7.2
NM_013230	CD24	CD24 molecule	-6.9
NM_000610	CD44	CD44 molecule (Indian blood group)	-2.0
NM_003507	Fzd7	Frizzled family receptor 7	-4.2
NM_000222	KIT	V-kit Hardy-Zuckerman 4 feline sarcoma viral oncogene homolog	-6.3
NM_002467	MYC	V-myc myelocytomatosis viral oncogene homolog (avian)	-2.6
NM_005430	Wnt1	Wingless-type MMTV integration site family, member 1	-6.3

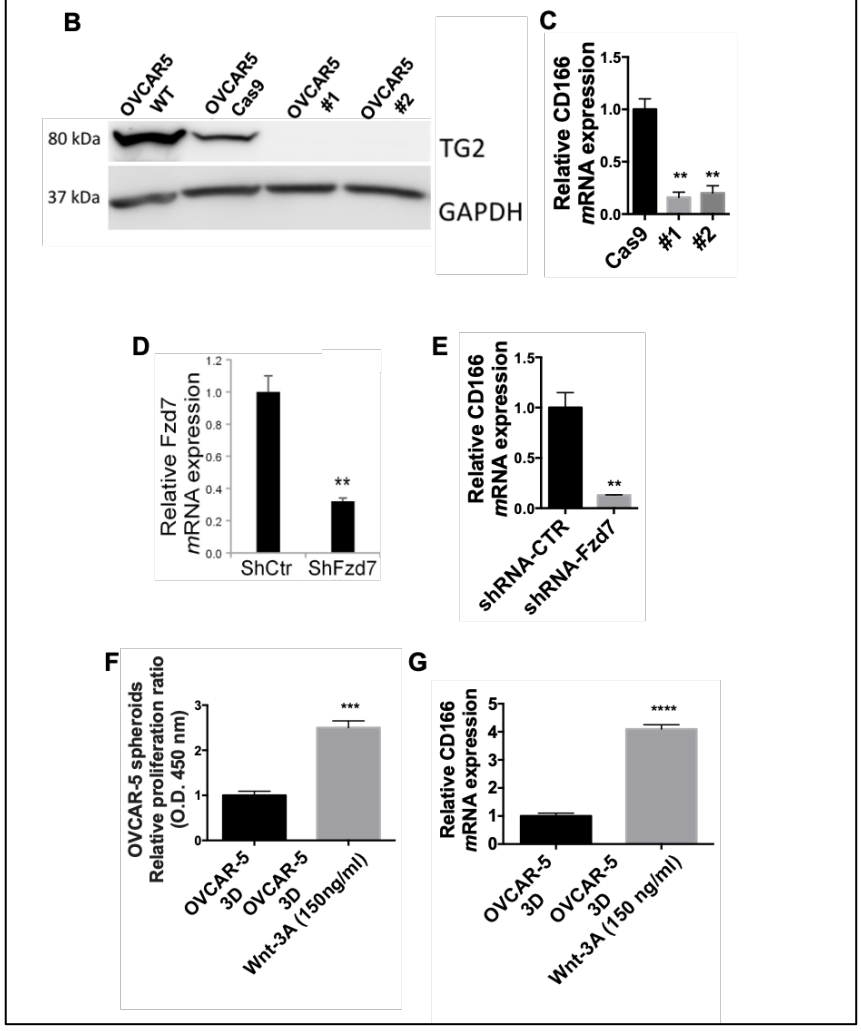

Figure 6. TG2/Fzd7 direct interaction regulates CD166 expression. A. List of CSC-related genes down-regulated in OVCAR-5 spheroids by 4G3 treatment compared to IgG control (≥2.0-fold change). **B.** Western blot shows TG2 expression levels in OVCAR5-WT cells compared to the TG2-KO clones 2D2 (#1) and 2H5 (#2). **C.** Real-time PCR for CD166 in OVCAR5 cells stably transduced with Cas9 or TG2 KO clones #1 and #2 (N=3; **P<0.01). **D-E.** Real-time PCR for Fzd7 and CD166 in OVCAR-5 cells stably transduced with scrambled- or Fzd7-targeting ShRNA (N=3; **P<0.01). **F.** Proliferation assay measured the number of cells growing as spheroids derived from OVCAR-5 cell lines after treatment with Wnt3A for 6 days compared with controls (N=3; ***P < 0.001). **G.** Real-time PCR for CD166 in OVCAR-5 cells grown as spheroids and treated with Wnt-3A (150 ng/ml) or control (N=3; ****P<0.0001).

IgG control cells(n = 3, P < 0.0001, Fig. 5A-D). AZN-L50 in combination with carboplatin was more effective in decreasing spheroids and colony formation compared to carboplatin alone treated cells (n = 3, P < 0.0001, Fig. A-D). In addition, OVCAR-8 cells CD166-KD were more sensitive to carboplatin treatment compared to CD166 expressing cells (Fig. 5E; n=3; **P<0.01; ****P<0.0001). Collectively, these data support that targeting of CD166 blocks OC cell proliferation and survival under 3D culture conditions and synergizes with chemotherapy.

TG2/Fzd7 interaction regulates CD166 expression in ovarian spheroid proliferation. We demonstrated that TG2, but also the other members of the ECM adhesion complex (FN and integrin β1) are enriched in OCSC and contribute to activation of the stemness-associated Wnt pathway by specifically engaging the Wnt receptor Fzd7. One of the main goals pursued during this funded project is to define the mechanism through which TG2/Fzd7 complex formation activates Wnt/β-catenin pathway promoting stemness associated genes expression in OCSCs. Our data showed a significant decrease in OC stemness related genes after 4G3-mediated TG2/Fzd7 complex disruption (Fig. 6A). One of the genes significantly downregulated was CD166 (Fig. 6A). In addition, TG2 CRISPR/Cas9 knock out (KO) (Fig. 6B) and Fzd7 shRNA-mediated KD OC cell lines (Hey-A8, OVCAR-5-8, SKOV3) showed a significant decrease in CD166 expression levels compared to shRNA transduced controls (OVCAR-5 data showed) (Fig 6C-D; N=3;

**P<0.01). The data led us to hypothesize that CD166 could be functionally linked to the tumorigenic OCSC phenotype and its expression in OC cells modulated by the oncogenic Wnt/β-catenin pathway. In this regard, we found that OC cell lines (Hey-A8, OVCAR-5-8, SKOV3) treated with the Wnt ligand Wnt-3A increased their proliferation ratio as spheroids compared to untreated controls (OVCAR-5 data showed) (Fig 6D; N=3; ***P<0.001). In parallel, the results showed a significant increase in CD166 expression levels after Wnt-3A treatment compared to untreated OVCAR-5 cells grown as spheroids (Fig 6E; N=3; ****P<0.0001). The data provided a strong rationale to investigate this molecule as a potential TG2/Fzd7 target gene and as a new therapeutic target in OC.

CD166 is a β-catenin target gene.

To investigate the mechanism by which the TG2/Fzd7 complex alters Wnt signaling, we tested the possibility that components of the complex directly interact with CD166. Both TG2 and Fzd7 were detected in endogenous protein lysates from OC cell lines pulled down with an anti-TG2 antibody (Fig. 7A) and anti-CD166 (Fig. 7B). To further define the interaction between TG2, Fzd7, and CD166 we used full-length recombinant TG2, CD166, and Fzd7 proteins. Co-IP with anti-TG2 antibody demonstrates direct interaction between TG2 and CD166 (Fig. 7C). Co-IP with anti-CD166 antibody demonstrates direct interaction between CD166 and Fzd7 (Fig. 7D).

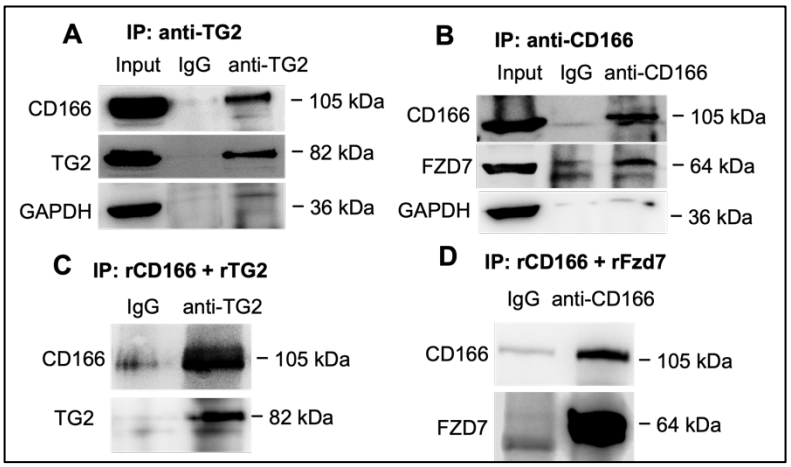

Figure 7. CD166 forms a complex with TG2 and Fzd7 in OC spheroids. A-B. Co-IP with anti-TG2 and anti-CD166 mAbs of cell lysates from OC spheroids. Western blotting was performed by using anti-Fzd7, CD166, TG2 and GAPDH antibodies. **C-D.** Co-IP with anti-TG2 and anti-CD166 mAbs and Western blotting for TG2, Fzd7 and CD166 using full-length recombinant TG2, CD166 and Fzd7.

TG2/Fzd7 complex formation increases Wnt/β-catenin signal transduction that in turn fuels a positive feedback loop. Having demonstrated a Wnt-3A mediated CD166 expression and a direct interaction of this molecule with TG2/Fzd7 complexes, we investigated whether CD166 is a β-catenin target gene.

To test this hypothesis, we measured CD166 mRNA expression levels after β-catenin knockdown. SiRNA-mediated β-catenin downregulation induced decreased CD166 expression, suggesting that CD166 is transcriptionally regulated by β-catenin (Fig. 8A; n=3; ***P<0.001; ****P<0.0001). To demonstrate definitively this concept, we searched and identified potential TCF/LEF responsive elements at positions (−93 to − 86) within the CD166 promoter sequence (Fig. 8B) by using a promoter motif searching software (PROMO). ChIP tested whether β-catenin interacts with the CD1661 promoter. Realtime-PCR amplified the CD166 promoter fragments corresponding to the TCF/LEF responsive regions in the chromatin pulled down by a β-catenin antibody (Fig. 8C). Specificity of β-catenin antibody binding to its target genes was demonstrated by observing amplification of b-catenin target gene c-Myc product (Fig. 8C). These data demonstrate that CD166 is a direct β-catenin target in OC cells.

CD166 and Wnt signaling regulate OC spheroids survival and proliferation

Initially, most tumors and ovarian cancer cell lines are platinum sensitive, but invariably, after repeated exposure, drug resistance develops, limiting clinical outcome. Much effort has been directed to understand the mechanisms involved in chemoresistance. It is becoming accepted that one of the important causes of platinum resistance relates to aberrant functioning of the apoptotic machinery in cancer cells, with both protein kinase B (Akt)- and focal adhesion kinase (FAK)-regulated survival pathways being implicated in acquired EOC platinum resistance. Further evidence indicates that CD166-CD166 interactions are crucial to the survival and primary site maintenance of cancer cells. In addition, CD166 gene silencing decreases the concentration of Bcl-2 and increases levels of apoptosis (poly(ADP-ribose) polymerase and active caspase-7; therefore, CD166 may also play an important role in protecting cancer cells against apoptosis. We investigated whether CD166 is linked with chemo resistance and apoptosis escape by sustained activation of survival signaling by FAK and AKT activation. Western blot analysis confirmed that HEY-A8 and OVCAR-8 cells grown as spheroids are enriched in CD166, active phospho-FAK and phospho-AKT expression compared to the same cells grown as monolayers (Fig. 9A). Sh-CD166 KD HEY-A8 cells grown as spheroids showed decreased phospho-FAK^{Tyr397} and phospho-AKT^{Ser473} activation compared to sh-Ctr cells (Fig. 9B). AKT phosphorylation in turn activated the anti-apoptotic signaling by inhibition of BAD through its phosphorylation at Ser112. This evidence prompted us to investigate the role of CD166 in survival pathway activation conferring chemoresistance. Sh-CD166 KD HEY-A8 cells increased response to platinum by decreasing the levels of phospho-FAK^{Tyr397} and phospho-AKT^{Ser473}. This in turn led to a decreased phospho-BAD^{Ser112} with a consequent pro-apoptotic phenotype through caspase 3 cleavage (Fig. 9C). We are currently linking this mechanism to TG2 and Fzd7 expression by using TG2- and Fzd7-KO cells treated or not with Wnt-3A. If confirmed, we propose that the TG2/Fzd7-mediated Wnt activation leads to CD166 expression, which in turn promotes cell-cell adhesion and apoptosis escape, proposing CD166 as target to block chemoresistance and tumorigenesis (Fig. 9D).

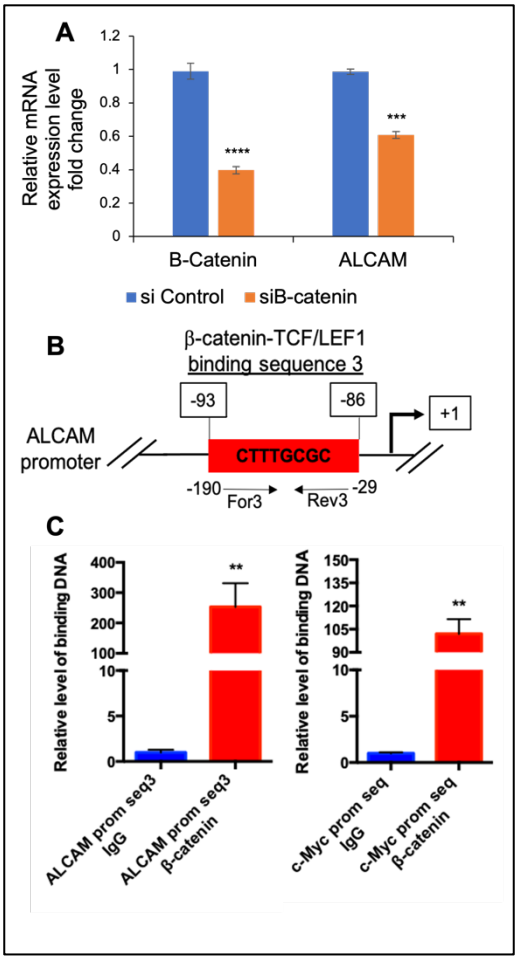

Figure 8. CD166 is a b-catenin target gene. A. Realtime–PCR for CD166 and β-catenin expression levels in HEY-A8 cells transfected with scrambled or β-catenin targeting siRNA (n=3; ***P<0.001; ****P<0.0001). **B.** Scheme representing the TCF/LEF1 binding sequences within the CD166 promoter relative to the designed primers. **C.** ChIP assay used chromatin from HEY-A8 cells immunoprecipitated with β-catenin or IgG (control). C-myc promoter-specific primers used as positive control (n=3; **P<0.01).

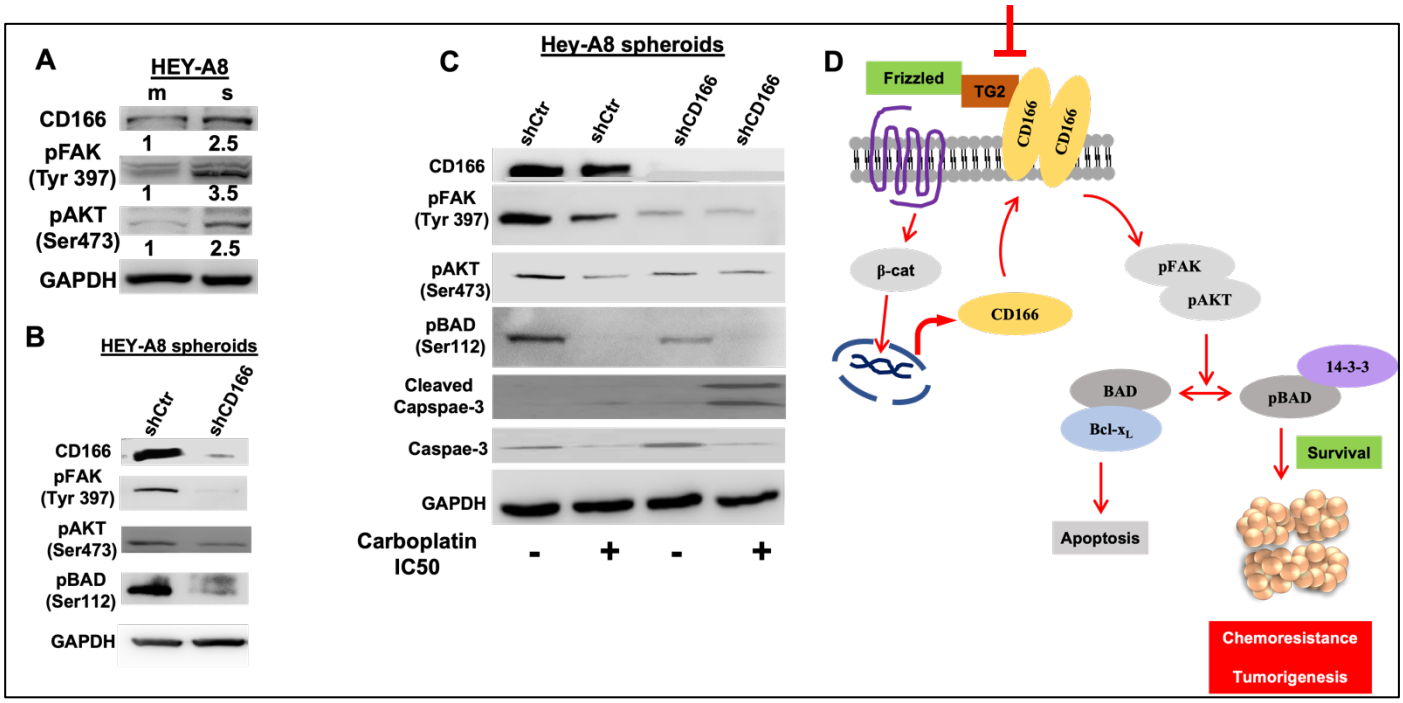

Figure 9: OC spheroids express CD166, active p-FAK and p-AKT. A. WB shows CD166, p-FAK^{Tyr397} and p-AKT^{Ser473} levels in HEY-A8 and OVCAR-8 grown as monolayers (m) and spheroids (s). Densitometry quantifies CD166, p-FAK^{Tyr397} and p-AKT^{Ser473} normalized for GAPDH. **B.** WB for CD166, phospho-FAK^{Tyr397}, phospho-AKT^{Ser473}, and phospho-BAD^{Ser112} in HEY-A8 cells stably transduced with scrambled- or CD166-targeting shRNA. **C.** WB for CD166, phospho-FAK^{Tyr397}, phospho-AKT^{Ser473}, phospho-BAD^{Ser112}, cleaved caspase-3 and caspase-3 in HEY-A8 cells stably transduced with scrambled- or CD166-targeting shRNA and treated or not with carboplatin IC50. **D.** Proposed mechanism.

Project 2: Tissue transglutaminase mediated integrin-linked kinase activation is a key regulator of Wnt/β-catenin signaling in ovarian cancer

Introduction: TG2 is overexpressed in ovarian tumors compared to normal ovarian epithelium and promotes enhanced peritoneal dissemination. Our recently published work demonstrated that expression of the FN binding domain of TG2 engages in a complex with the Wnt-receptor Frizzled 7 leading to β-catenin signaling, which in turn promotes ovarian cancer cell proliferation and a cancer stem-like cell phenotype. Further evidence demonstrates that in the context of cell-matrix interactions and through recruitment of Src kinase, TG2 regulates ovarian cancer cell proliferation, interconnecting the integrin and β-catenin pathways. The complexity of pathological and physiological roles regulated by Wnt signaling and the crosstalk with other major pathways, underlies the difficulties in finding an effective therapeutic agent against this pathway. Thus, highlighting the necessity of targeting molecules associated with Wnt signaling as a therapeutic strategy. The goal of our study was to analyze the mechanism by which TG2 interactions with ECM led to β-catenin signaling. Here, we demonstrated that TG2 mediated outside in molecular responses by phosphorylating the integrin linked kinase (ILK) at Ser^{246}. ILK activation inhibited its downstream effector, glycogen synthase kinase-3α/β (GSK-3α/β), leading to β-catenin nuclear translocation in OC cells. Complexes formation between TG2 and the active phospho-ILK at Ser^{246} were ECM substrate dependent and were highly enriched in patient-derived OC primary cells grown on FN-coated slides compared with cells plated on glass alone. ILK expression

was strongly correlated with TGM2 (R=0.1, P < 0.0001), ITGB1 (R=0.1, P < 0.001), and with FN1 (R =0.2, P < 0.0001) in the TCGA OC database. Use of function-inhibiting antibody against the FN-binding domain of TG2 (clone 4G3) and the ILK small molecule inhibitor, cpd-22, suppressed ILK activation and in turn the canonical Wnt/β-catenin signaling. By demonstrating that TG2 regulates directly ILK activation, we defined a new mechanism linking ECM cues with Wnt/β-catenin signaling in OC tumorigenesis. The results point to the central role of TG2/FN/integrin clusters in ECM re-arrangement and propose its downstream effector ILK as potential new therapeutic target in OC.

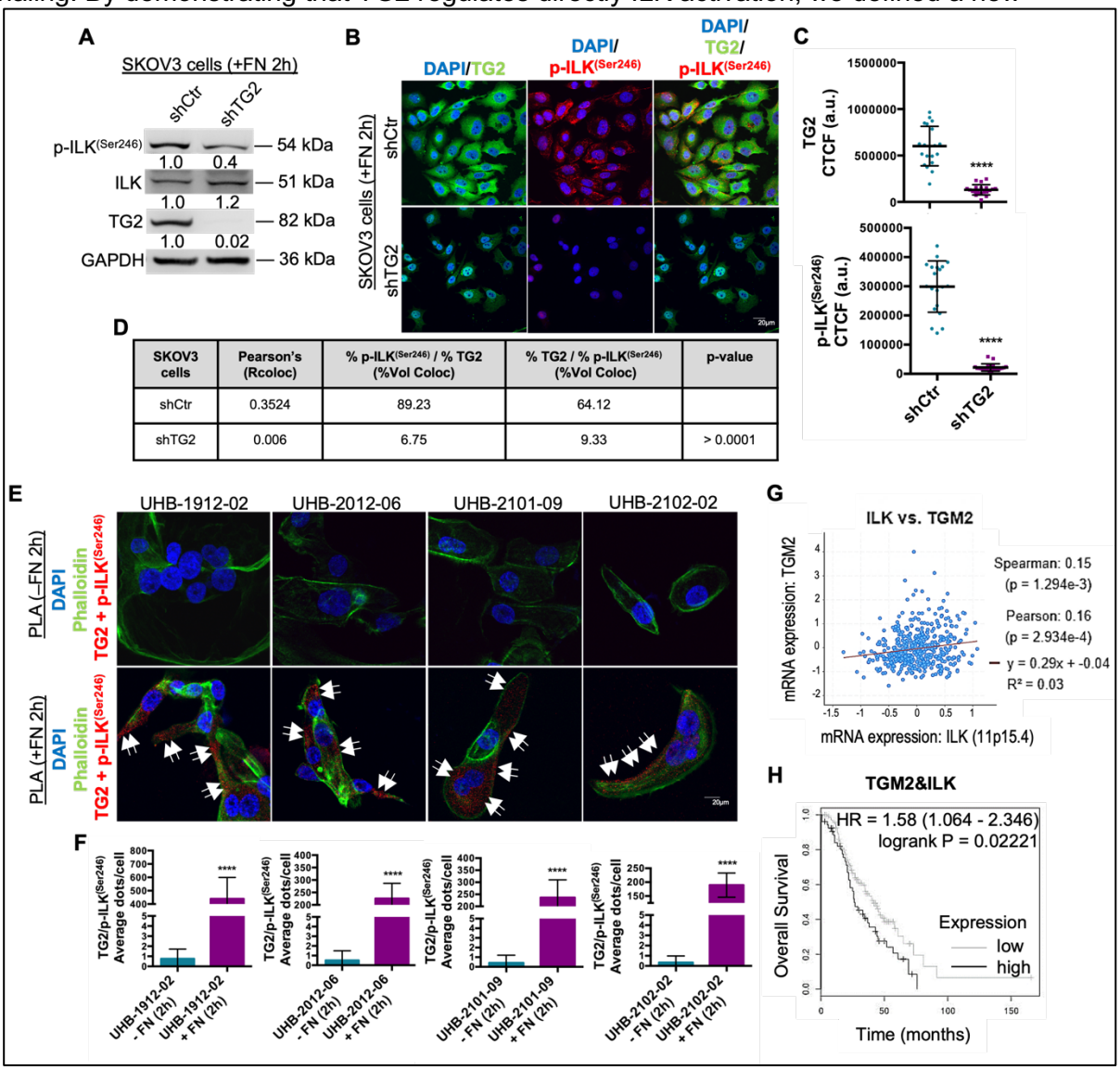

Figure 10: TG2 expression activates ILK in OC cells. A. WB for p-ILK^{Ser246}, ILK, and TG2 in SKOV3 cells stably transduced with scrambled- or TG2-targeting shRNA. Densitometry quantifies TG2, p-ILK^{Ser246}, ILK expression levels normalized for GAPDH. **B.** Immunofluorescence staining for TG2 (Alexa Fluor 488, green) and p-ILK^{Ser246} (Alexa Fluor 568, red) in SKOV3 cells sh-Ctr or sh-TG2 KD. Protein colocalization is identified by yellow spectra on merged images. **C.** Quantification of Alexa Fluor 488 (green) and Alexa Fluor 568 (red) proteins was calculated by using Metamorph software (N= 3; P < 0.0001). **D.** Quantification of colocalized proteins was calculated by volume area of green over red spectra in sh-control (N = 3; Pearson's rank correlation = 0.3) versus sh-TG2 SKOV3 cells (N = 3; Pearson's rank correlation = 0.006; P<0.0001). **E.** TG2/p-ILK^{Ser246}colocalization (red dots) and phalloidin (green) detected by PLA in 4 primary human cells isolated from de-identified malignant ascites fluid specimens and plated on plastic or FN-coated plates. Representative images are shown (magnification, X 200). Bar, 20 μm. **F.** Quantification of the number of total TG2/p-ILK^{Ser246} red dots per sample in a diagram (N= 3; P<0.0001). **G.** Correlation between TG2 and ILK mRNA expression levels (Spearman r = 0.15, P = 1.2e-3 and Pearson r = 0.15, P = 2.9e-4; Fig. 1G) in the TCGA ovarian cancer database obtained from cBioPortal. **H.** Overall survival curves generated using the Kaplan–Meier plot for tumors expressing high levels of TG2 and of ILK versus those expressing low levels of TG2 and of ILK in HGSOC tumor microarray data of 14 datasets from 7 different array platforms using OvMark (P = 0.02).

Results:

We investigated whether TG2 mediated FN-integrins cluster formation was sufficient to transduce the outside in signaling by phospho-ILK^{Ser246} in OC

cells. SKOV3 and OVCAR-5 cells were transduced with an empty viral vector control (sh-Ctr) or knocked down (KD) with an sh-RNA targeting TG2 (sh-TG2) and plated on plastic or FN-coated plates for 2 h. Western blot analyses revealed that phospho-ILK^{Ser246} levels decreased by ~ 2.5-fold in sh-TG2 SKOV3 (Fig. 10A) and OVCAR-5 cells (not shown) compared to the sh-Ctr cells grown on FN. Of interest, OC cells grown on plastic showed a weak basal level of phospho-ILK^{Ser246} and no significant differences were observed in TG2 expressing OC cells compared to sh-TG2 cells (not shown). In addition, no significant changes were observed in the total ILK expression in sh-TG2 compared to sh-Ctr OC cells (Figs. 10A).

IF microscopy and intensity profile analysis confirmed a significantly increased signal for phospho-ILK^{Ser246} staining in OC cells sh-Ctr compared to sh-TG2 cells (Fig. 10B-C; $P < 0.0001$) plated on FN. IF confocal and co-localization analysis showed that TG2 and phopho-ILK^{Ser246} were significantly co-localized on the cell membrane and in invadopodia in sh-Ctr SKOV3 (Rcoloc = 0.35) plated on FN compared to sh-TG2 SKOV3 (Rcoloc = 0.006, $P < 0.0001$) (Fig. 10D). The data confirmed that ILK activation is ECM substrate dependent and functionally regulated by TG2 expression in OC cells.

Next, to determine whether TG2-phospho-ILK(Ser246) clusters are detectable in human tumors, we used proximity ligation assay (PLA), a technique capable of identifying proteins localized within 40 nm distance in tissue. TG2 and phospho-ILKSer^{246} expression and colocalization were measured on 4 primary human cells isolated from de-identified malignant ascites fluid specimens and plated on plastic or FN-coated plates. TG2-phospho-ILK^{Ser246} complex formation was detectable on cell membrane

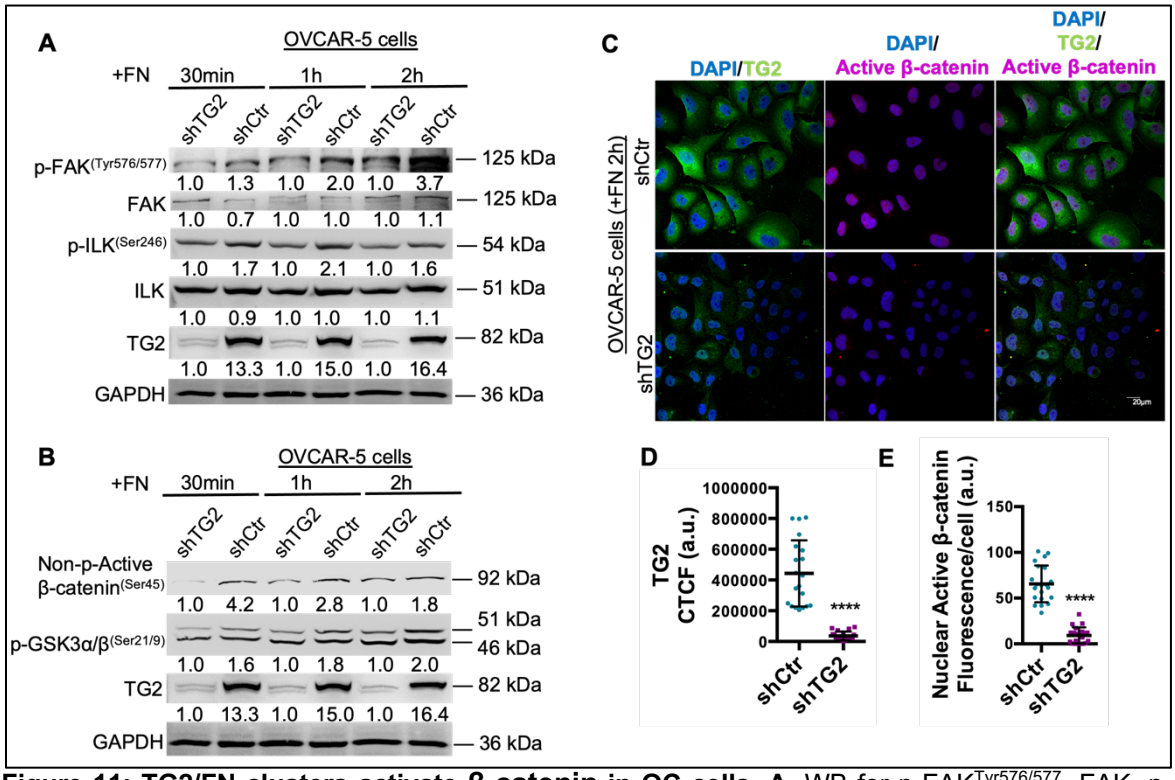

Figure 11: TG2/FN clusters activate β-catenin in OC cells. A. WB for p-FAK$^{Tyr576/577}$, FAK, p-ILK^{Ser246}, ILK, and TG2 in OVCAR-5 cells stably transduced with scrambled- or TG2-targeting shRNA and plated on FN coated plates for 30 min, 1, h, and 2h. Densitometry quantifies p-FAK$^{Tyr576/577}$, FAK, p-ILK^{Ser246}, ILK, and TG2 expression levels normalized for GAPDH. **B.** WB for non-p-active β-catenin^{Ser45} and p-GSKα/β$^{Ser21/9}$ in OVCAR-5 cells stably transduced with scrambled- or TG2-targeting shRNA and plated on FN coated plates for 30 min, 1, h, and 2h. Densitometry quantifies non-p-active β-catenin and p-GSKα/β$^{Ser21/9}$ expression levels normalized for GAPDH. **C.** Immunofluorescence staining for TG2 (Alexa Fluor 488, green) and non-p-active β-catenin^{Ser45} (Alexa Fluor 568, red) in OVCAR-5 cells sh-Ctr or sh-TG2 KD plated on FN for 2 h. **D-E.** Quantification of Alexa Fluor 488 (green) and Alexa Fluor 568 (red) proteins was calculated by using Metamorph software (N= 3; $P < 0.0001$).

and in invadopodia in all of 4 ovarian malignant tumor cells plated on FN, but not in primary OC cells plated on plastic (Fig. 10E-F; $P < 0.0001$), supporting a functional interaction between the two proteins in malignant cells in vivo. The results point to the central role of TG2 in the activation of the downstream effector phospho-ILK^{Ser246} in OC cells.

In addition, analysis of 489 clinically annotated HGSOC tumors in the TCGA ovarian cancer database were obtained from cBioPortal. ILK expression was strongly correlated with TG2 (Spearman r = 0.15, P = 1.2e-3 and Pearson r = 0.15, P = 2.9e-4; Fig. 10G). Furthermore, analysis of HGSOC tumor microarray data of 14 datasets from 7 different array platforms using OvMark demonstrated that patients with high TG2 and ILK expression levels had an increased estimated risk of death when compared with those with low TG2 and ILK expression levels (Fig. 10H). These data support the significance of ILK as effector of ECM processes in human ovarian tumors affecting clinical outcomes.

TG2–FN interaction activates ILK and mediates β-catenin nuclear translocation

The Wnt/β-catenin signaling is an evolutionarily conserved pathway that determines the fate decisions of the cells and tissue modeling during embryonic development. Mutations in the β-catenin gene (*CTNNB1),* loss-of-function mutations in the β-catenin destruction complex (*APC* and *Axin),* or upregulation of Wnt receptors and ligands lead to the aberrant activation and nuclear localization of β-catenin and correlate with OC tumor progression. In previous reports, we demonstrated that in the context of cell-matrix interactions TG2 regulates β-catenin signaling. To understand the consequences of TG2-induced ILK phosphorylation at Ser^{246} in cell-matrix interactions, activation of β-catenin was measured in OC cells plated on FN matrices. First, we confirmed an increase in phospho-ILK^{Ser246} and observed an activation of focal adhesion complexes by measuring phosphorylation of FAK at Tyr$^{576/577}$ in OVCAR-5/sh-Ctr plated on FN compared to sh-TG2 cells (Fig. 11A). Focal adhesion assembly is an early event. In our experiments, ILK activation and FAK phosphorylation at Tyr$^{576/577}$ occurred 30 min upon cell adhesion to FN and the regulatory signal remained active for up to 2 h. Increased ILK and FAK phosphorylation in sh-Ctr OC cells correlated with phosphorylation of GSK-3α/β at Ser$^{21/9}$ (Fig. 11B). In cell rest state, GSK-3α/β phosphorylates β-catenin at Ser$^{33/37}$/Thr^{41}, triggering its destabilization and subsequent ubiquitin-proteasome mediated degradation. Upon Wnt activation, GSK-3α/β is phosphorylated and inactivated at Ser$^{21/9}$ resulting in the suppression of β-catenin phosphorylation at Ser$^{33/37}$/Thr^{41} and in its stabilization. By using a monoclonal antibody directed against the non-phospho (active) β-catenin at Ser$^{33/37}$/Thr^{41}, sh-Ctr/OVCAR-5 cells showed increased active β-catenin levels compared to sh-TG2 cells (Fig. 11B).

IF microscopy and intensity profile analysis confirmed the TG2-KD in sh-TG2 transduced cells and a significant depletion of nuclear translocation of active β-catenin compared to sh-Ctr OC cells (Fig. 11C-E; $P < 0.0001$) plated on FN for 2 h. The data indicate that TG2 expression is essential to translate extracellular cues into oncogenic β-catenin signaling by modulating ILK activation.

ILK inhibition blocks β-catenin signaling

To determine whether ILK activation is essential to promote β-catenin nuclear translocation, we modulated ILK activity in OC cells by either sh-RNA mediated KD or pharmacological inhibition. The tri-substituted pyrazol compound 22 is a specific cell-permeable ILK inhibitor (IC50 = 600 nM) with high anti-proliferative potency against prostate and breast cancer cell lines (IC50 = 1 to 2.5 μM) while normal epithelial cells are not affected. OVCAR-5 cells were plated on FN for 2 h in the presence of Wnt-3A (150 ng/ml) and/or cpd-22 at 0.5 μM or 1 μM. We observed an increase in both phospho-FAK$^{Tyr576/577}$ and phospho-ILK^{Ser246} levels induced by Wnt-3A compared to DMSO control cells (Fig. 12A). Cpd-22 treatment effectively reduced the phosphorylation levels of both proteins in the Wnt-3A groups, while no significant changes were observed at the basal level compared to DMSO control cells (Fig. 12A). Total FAK and ILK expression

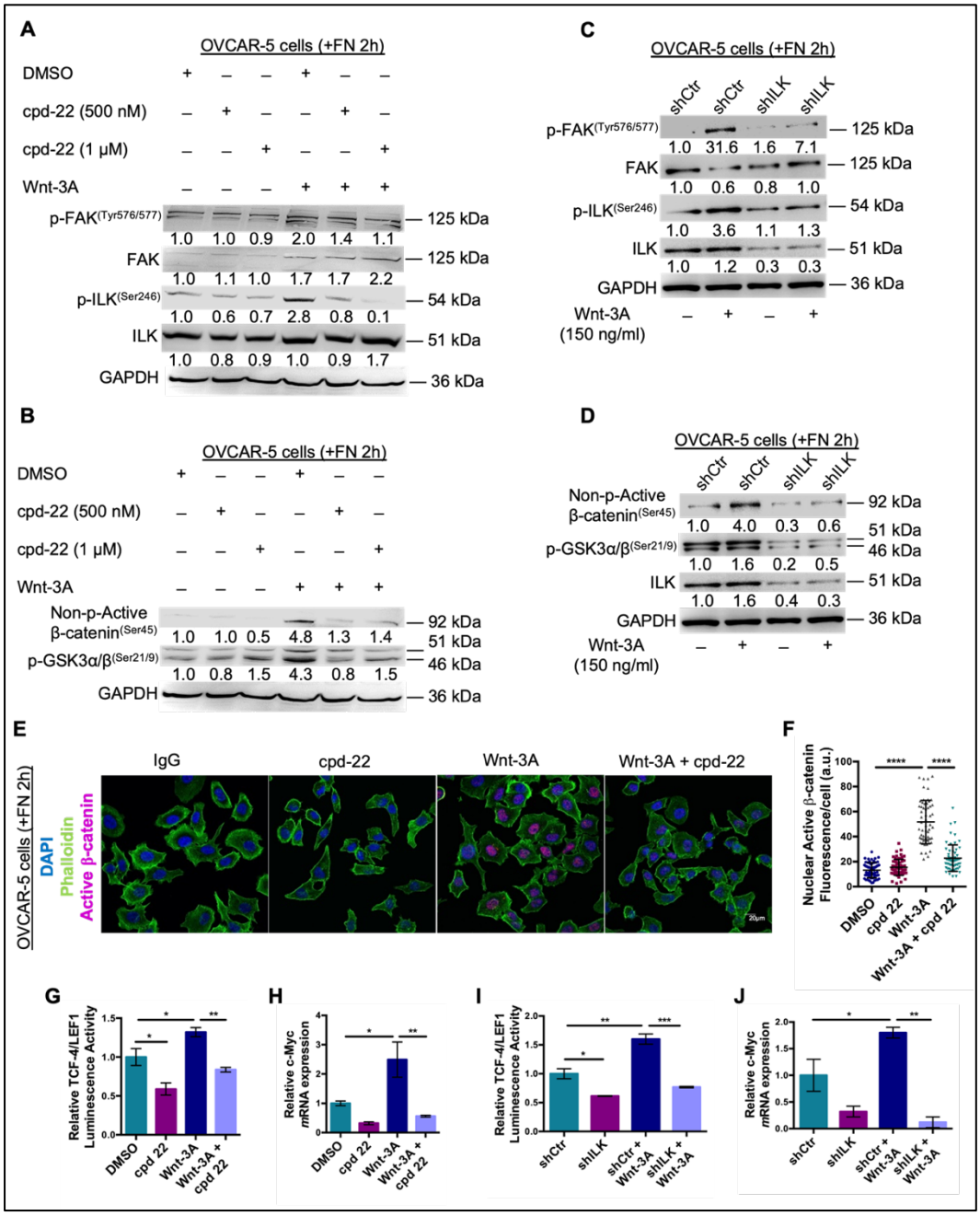

Figure 12: ILK inhibition blocks β-catenin signaling in OC cells. A-B. WB for p-FAK$^{Tyr576/577}$, FAK, p-ILK^{Ser246}, ILK, non-p-active β-catenin^{Ser45} and p-GSKα/β$^{Ser21/9}$ in OVCAR-5 cells plated on FN coated plates for 2 h and treated or not with cpd-22 and/or Wnt-3A. Densitometry quantifies proteins expression levels normalized for GAPDH. **C-D.** WB for p-FAK$^{Tyr576/577}$, FAK, p-ILK^{Ser246}, ILK, non-p-active β-catenin^{Ser45} and p-GSKα/β$^{Ser21/9}$ in OVCAR-5 cells sh-Ctr or sh-ILK plated on FN for 2 h and treated or not with Wnt-3A. Densitometry quantifies proteins expression levels normalized for GAPDH. **E.** Immunofluorescence staining for phalloidin (Alexa Fluor 488, green) and non-p-active β-catenin^{Ser45} (Alexa Fluor 568, red) in OVCAR-5 cells plated on FN coated plates for 2 h and treated or not with cpd-22 and/or Wnt-3A. **F.** Quantification of Alexa Fluor 568 (red) proteins was calculated by using Metamorph software (N= 3; P < 0.0001). **G.** OVCAR5 cells were co-transfected with TCF/LEF1 luciferase reporter and Renilla control plasmid prior to treatment with cpd-22 or Wnt-3A and plated on FN for 2 h. Luciferase signal relative to Renilla activity is expressed as fold increase (N = 6; *P < 0.05; **P < 0.01). **H.** Realtime PCR for c-Myc in OVCAR-5 cells plated on FN coated plates for 2 h and treated or not with cpd-22 and/or Wnt-3A (N=6; *P < 0.05; **P < 0.01). **I.** OVCAR5 cells sh-Ctr or sh-ILK were co-transfected with TCF/LEF1 luciferase reporter and Renilla control plasmid prior to treatment with cpd-22 or Wnt-3A and plated on FN for 2 h (N = 6; *P < 0.05; **P < 0.01; ***P<0.001). **J.** Real-time PCR for c-Myc in OVCAR-5 cells stably transduced with scrambled- or ILK-targeting shRNA plated on FN coated plates for 2 h and treated or not with Wnt-3A (N=6; *P < 0.05; **P < 0.01).

levels were not altered by Wnt-3A or cpd-22 treatment (Fig. 12A). Wnt-3A treatment showed ~ 4.3-fold increase in the inhibitory phosphorylation of GSK-3α/β at $Ser^{21/9}$ with a consequent ~ 4.8-fold increase in non-phospho (active) β-$catenin^{Ser33/37/Thr41}$ levels compared to control OVCAR-5 cells (Fig. 12B). Cpd-22 treatment drastically reduced the inhibitory phosphorylation of GSK-3α/β at $Ser^{21/9}$ and the non-phospho (active) β-$catenin^{Ser33/37/Thr41)}$ (Fig. 12B). To confirm the data observed with ILK pharmacological inhibition, we transduced OVCAR-5 with sh-RNA targeting ILK or sh-RNA Ctr. Efficient ILK-KD in OC cells versus control (scrambled) siRNA was achieved (Fig. 12C). Western blot analysis showed that Wnt-3A increased phospho-$FAK^{Tyr576/577}$ and phospho-ILK^{Ser246} expression in ILK- expressing cells compared with that in low-ILK-expressing cells (Fig. 12C). Consistent with these observations, ILK downregulation blocked the Wnt-3A mediated phosphorylation of GSK-3α/β at $Ser^{21/9}$ and subsequent non-phospho (active) β-$catenin^{Ser33/37/Thr41}$ levels in both OVCAR-5/sh-ILK cells compared to OVCAR-5/sh-Ctr cells (Fig. 12D), suggesting that the ILK stabilizes the focal adhesion contacts and the β-catenin signaling in TG2 expressing OC cells.

Next, IF microscopy and intensity profile analysis detected a significantly stronger non-phospho (active) β-catenin at ($Ser^{33/37}$/Thr^{41}) nuclear translocation in OVCAR-5 cells treated with Wnt-3A compared to untreated control cells, whereas treatment with cpd-22 at 0.5 μM blocked the non-phospho (active) β-catenin nuclear translocation in OC cells (Fig. 12E-F; $P < 0.0001$). ILK inhibitor cpd-22 significantly reduced the Wnt-3A mediated β-catenin/TCF transcriptional activity as measured by TCF/LEF1 reporter assay in OVCAR5 cells ($n = 3$, $P < 0.05$, $P < 0.01$; Fig. 12G). In addition, cpd-22 treatment decreased the β-catenin target gene c-Myc mRNA levels in both OC cell lines ($n = 3$, $P < 0.05$, $P < 0.01$; Fig. 12H). To support these observation, ILK-KD significantly reduced the Wnt-3A mediated β-catenin/TCF transcriptional activity in OVCAR5-sh-ILK cells ($n = 3$, $P < 0.05$, $P < 0.01$, $P < 0.001$; Fig. 12I) and decreased the β-catenin target gene c-Myc mRNA levels ($n = 3$, $P < 0.05$, $P < 0.01$; Fig. 12J) compared to OVCAR5/sh-Ctr cells.

TG2-FN interaction stimulates OC cell proliferation and migration through ILK activation

TG2 expression increases adhesion to FN causing integrin aggregation, which is turn translates extracellular cues into β-catenin transcriptional activity by modulating a crosstalk with ILK. Here, we evaluated whether the TG-FN dependent activation of ILK supports the ovarian cancer proliferation and progression by translating the outside in signaling into the oncogenic Wnt pathway.

To test this, OC cells were plated on FN-coated surfaces and treated with Wnt-3A and/or anti-TG2 inhibitory mAb (clone 4G3). Proliferation (CCK-8 assay) and migration assays were measured. OC cells treated with 4G3 adhered less efficiently to the matrix and as consequence showed decreased proliferation and migration rates compared to IgG control cells (Fig. 13A-B; $P < 0.0001$). Wnt-3a treatment efficiently increased proliferation and migration in both OC cells compared to IgG control, whereas 4G3 treatment drastically reduced Wnt-3A effects (Fig. 13A-B; $P < 0.0001$).

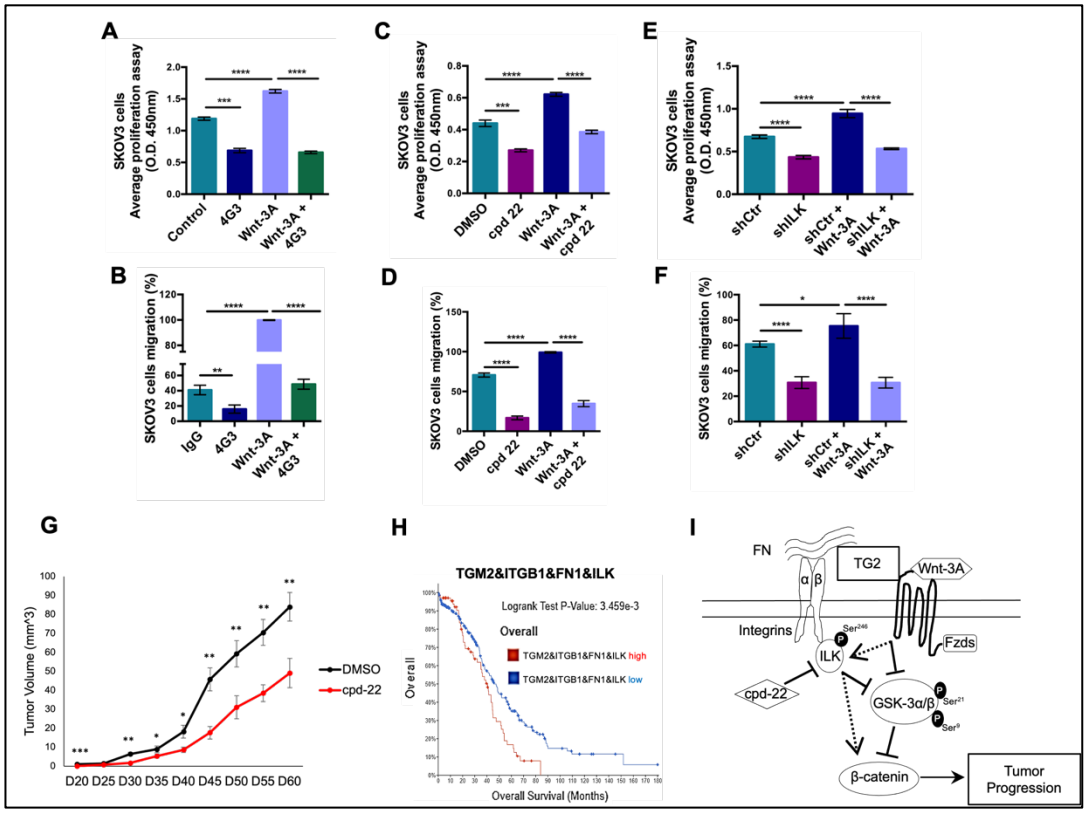

Figure 13: ILK functional inhibition in OVCAR-5 cells results in tumor growth inhibition. **A.** CCK-8 assay quantifies proliferation of SKOV3 cells treated with inhibitory mAbs directed against the FN-binding domain of TG2 (clone 4G3) and/or Wnt-3A (N=8; ***P<0.001; ****P<0.0001). **B.** Scratch assay quantifies migration of SKOV3 cells treated with 4G3 and/or Wnt-3A (N=8; **P<0.01; ****P<0.0001). **C.** CCK-8 assay quantifies proliferation of SKOV3 cells treated with cpd-22 and/or Wnt-3A (N=8; ***P<0.001; ****P<0.0001). **D.** Scratch assay quantifies migration of SKOV3 cells treated with cpd-22 and/or Wnt-3A (N=8; **P<0.01; ****P<0.0001). **E.** CCK-8 assay quantifies proliferation of ILK-KD vs sh-Ctr SKOV3 cells treated with or not with Wnt-3A (N=8; ****P<0.0001). **F.** Scratch assay quantifies migration of ILK-KD vs sh-Ctr SKOV3 cells treated with or not with Wnt-3A (N=8; *P<0.05; ****P < 0.0001). **G.** Tumor volumes derived from OVCAR-5 cells treated ex vivo with cpd-22 or DMSO control and injected subcutaneously in nude mice, as described (N=5; *P<0.05; **P<0.01; ***P<0.001). **H.** Overall survival curves generated using the Kaplan–Meier plot for tumors expressing high levels of TGM2, ITGB, FN1 and of ILK versus those expressing low levels of TGM2, ITGB, FN1 and of ILK in HGSOC tumor microarray (P=3.459e-3). **I.** Proposed mechanistic model.

To evaluate whether ILK mediated β-catenin signaling is implicated in the proliferation and migration of TG2-expressing cells on FN, we modulated ILK activity by pharmacological inhibition. Wnt-3A increased OC cells proliferation and migration rates of ~ 2- and 1.5-fold compared to DMSO control cells, whereas treatment with the ILK inhibitor cpd-22 decreased both proliferation and migration rates ~ 1.5- and 5-fold compared with DMSO control and after Wnt-3A treatment ~ 1.5- and 2.5-fold, respectively, in both cell lines, thus eliminating the input triggered by the TG2-FN interactions on β-catenin signaling (n = 3, P < 0.01, P < 0.0001; Fig. 13C-D). To further demonstrate that FN-stimulated OC cell proliferation and migration is regulated by ILK mediated β-catenin signaling, we used OC cells transduced with an empty lentiviral vector control (sh-Ctr) or an shRNA targeting ILK (sh-ILK). CCK-8 assay demonstrated decreased cell proliferation of FN-plated SKOV3/sh-ILK cells compared to control shRNA and after Wnt-3A treatment (n = 3, P < 0.01, P < 0.0001; Fig. 13C). Phase contrast microscopy and migration assay showed that sh-RNA mediated ILK-KD diminished OC cell migration on FN coated plates relative to cells transduced with sh-RNA Ctr and upon Wnt-3A treatment (n = 3, P < 0.0001; Fig. 13D, F). TG2-mediated ECM re-arrangement has been correlated with oncogenic pathway activation and tumorigenicity. Here, we treated 1 X10^6 OVCAR-5 cells ex vivo with 500 nM cpd-22 for 72 h before subcutaneous inoculation into the flanks of female nu/nu mice. Tumor growth was monitored. ILK functional inhibition resulted in slower tumor uptake and growth (cpd-22-treated OVCAR-5

cells; n = 5, *P<0.05; **P<0.01; ***P < 0.001; Fig. 13G), confirming the observation made in vitro. Analysis of 304 HGSOC tumor mRNA RNASeqv2 data obtained from cBioPortal demonstrated that patients with high TG2, ILK, ITGB1 (integrin β1), and FN1 (fibronectin) expression levels had an increased estimated risk of death when compared with those with low expression levels (Fig. 13H), supporting the proposed correlation between TG2-FN interaction, ILK activation and increased β-catenin transcriptional activity regulating cancer cell proliferation and tumorigenicity (Fig. 13I).

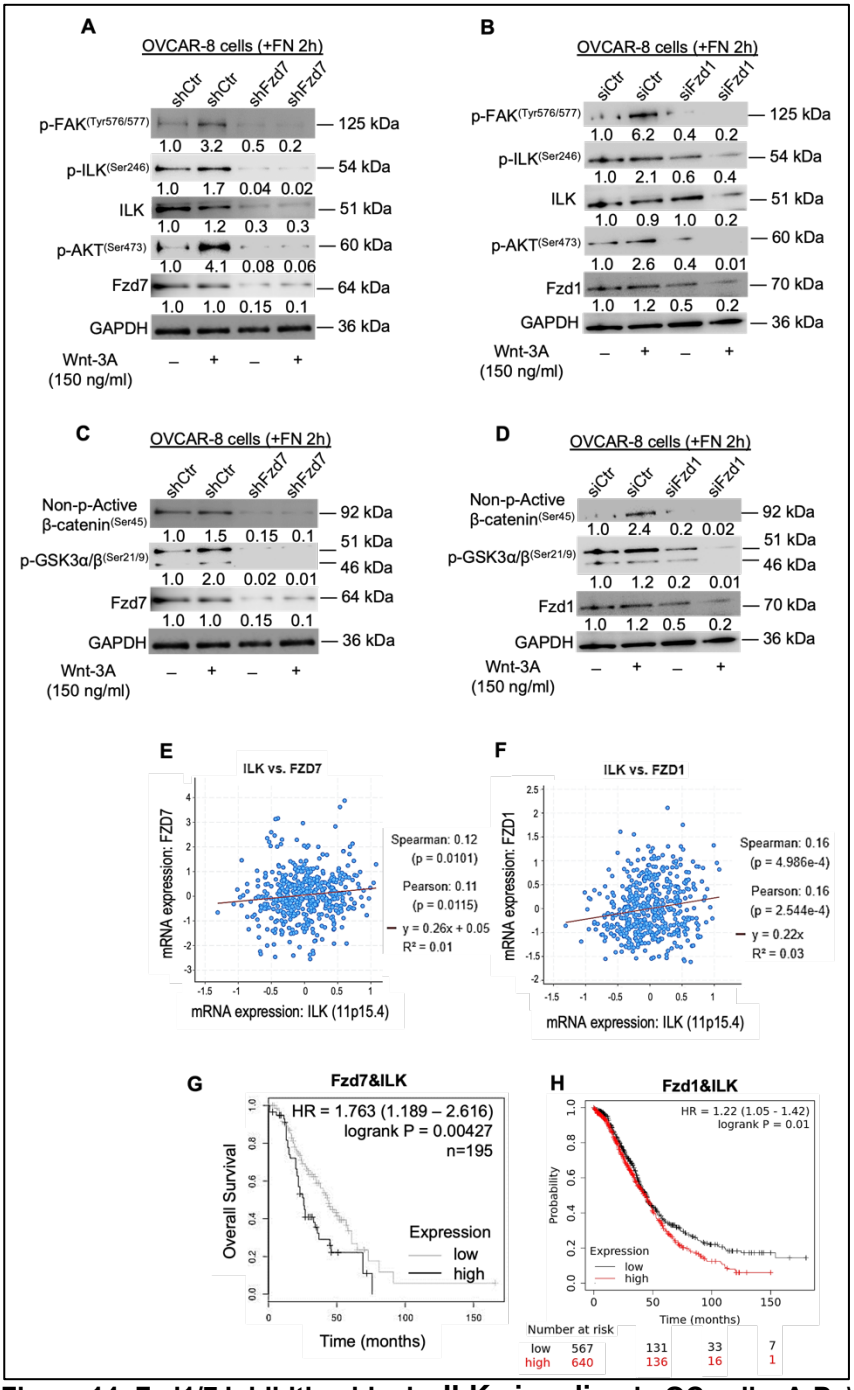

Figure 14: Fzd1/7 inhibition blocks ILK signaling in OC cells. A-D. WB for p-FAK$^{Tyr576/577}$, FAK, p-ILK^{Ser246}, ILK, Fzd1/7, non-p-active β-catenin^{Ser45} and p-GSKα/β$^{Ser21/9}$ in OVCAR-5 Fzd1/7 KD or control cells plated on FN coated plates for 2 h and treated or not with Wnt-3A. Densitometry quantifies p-FAK$^{Tyr576/577}$, FAK, p-ILK^{Ser246}, ILK, Fzd1/7, non-p-active β-catenin^{Ser45} and p-GSKα/β$^{Ser21/9}$ expression levels normalized for GAPDH. **E-F.** Correlation between Fzd7, Fzd1 and ILK mRNA expression levels in the TCGA ovarian cancer database obtained from cBioPortal. **G-H.** Overall survival curves generated using the Kaplan–Meier plot for tumors expressing high levels of Fzd7, Fzd1 and of ILK versus those expressing low levels of Fzd7, Fzd1 and of ILK in HGSOC tumor microarray.

Wnt receptors Fzd1 and 7 regulate focal adhesion by altering FAK and ILK expression and activity

We further showed that the Wnt receptors Fzd1 and 7 regulate ILK expression, suggesting the presence of a positive feedback loop between TG2, Wnt-3a, ILK, Fzd1 and Fzd7.

OVCAR-5 cells (showed) were transfected with siRNA targeting ILK or siRNA Ctr. Efficient Fzd1 and 7-KD in OC cells versus control (scrambled) siRNA was achieved (Fig. 14A-B). Western blot analysis showed that Wnt-3A increased phospho-FAK$^{Tyr576/577}$ and phospho-ILK^{Ser246} expression in Fzd1/7-expressing cells compared with that in Fzd1/7 KD-cells (Fig. 14A-B). Consistent with Fzd1/7 role in regulating the Wnt canonical pathway, Fzd1/7 downregulation blocked the Wnt-3A mediated phosphorylation of GSK-3α/β at Ser$^{21/9}$ and subsequent non-phospho (active) β-catenin$^{Ser33/37/Thr41}$ levels compared to OVCAR-5/siCtr cells (Fig. 14C-D).

In addition, analysis of 489 clinically annotated HGSOC tumors in the TCGA ovarian cancer database were obtained from cBioPortal. ILK expression was strongly correlated with those of both Fzd7 (Spearman r = 0.12,

P = 0.01 and Pearson r = 0.11, P = 0.01; Fig. 3H) and Fzd1 (Spearman r = 0.16, P = 4.9e-4 and Pearson r = 0.16, P = 2.5e-4; Fig. 14E-F). Furthermore, analysis of 1,200 HGSOC tumor array using Kaplan Meier plotter demonstrated that patients with high Fzd7 and ILK had a worse overall survival rate compared to those with low-expressing Fzd7 and ILK (Fig. 14G). In agreement with the previous data, analysis of HGSOC tumor microarray data of 14 datasets from 7 different array platforms using OvMark demonstrated that patients with high Fzd1 and ILK expression levels had an increased estimated risk of death when compared with those with low Fzd1 and ILK expression levels (Fig. 14H). These data support the significance of ILK as effector of ECM processes in human ovarian tumors affecting clinical outcomes.

Conclusions: Here we show that upon promoting ovarian cancer cell adhesion to FN matrices, TG2 mediates ILK phosphorylation at Ser^{246}, which in turn phosphorylates and inhibits its downstream effector GSK-3α/β at $Ser^{21/9}$, thereby, amplifying β-catenin signaling. TG2, Fzd1 and 7 form functional clusters with ILK at the cell surface in primary human ovarian cancer cells. Gene expression analysis from 489 patients in The Cancer Genome Atlas (TCGA) ovarian cancer data set demonstrates decreased overall survival when high TG2, Fzd1 or IFzd7 mRNA levels are co-expressed with those of ILK. In addition, functional inhibition and transcriptional downregulation of TG2, Fzd1-7 and ILK block cell adhesion to the matrix, Wnt response to the Wnt-3A ligand, and ultimately cell adhesion, migration and growth.

In conclusion, this report defines a new functional link between the TG2 regulated cell adhesion to the matrix, Fzd1 and 7 engagement and ILK phosphorylation with the canonical Wnt signaling activation, proposing ILK as a central node of two combinatorial signals and as a possible therapeutic target. (Article ready for submission).

Future steps:

TG2/ILK and Fzds/ILK clusters are enriched in chemo-resistant HGSOC cells compared to chemo-sensitive wild-type OC cells (Fig. 15) (experiments are ongoing). In addition, analysis of 1,200 HGSOC tumor array using Kaplan Meier plotter in patients treated with platin demonstrated that high TG2, Fzd1/7, β-catenin (CTNNB1) in correlation with ILK expression levels had a worse overall survival rate compared to those with low-expressing proteins (Fig. 15). The preliminary data further validate the functional importance of these clusters at the interface with the tumor stroma in regulating the oncogenic Wnt signaling.

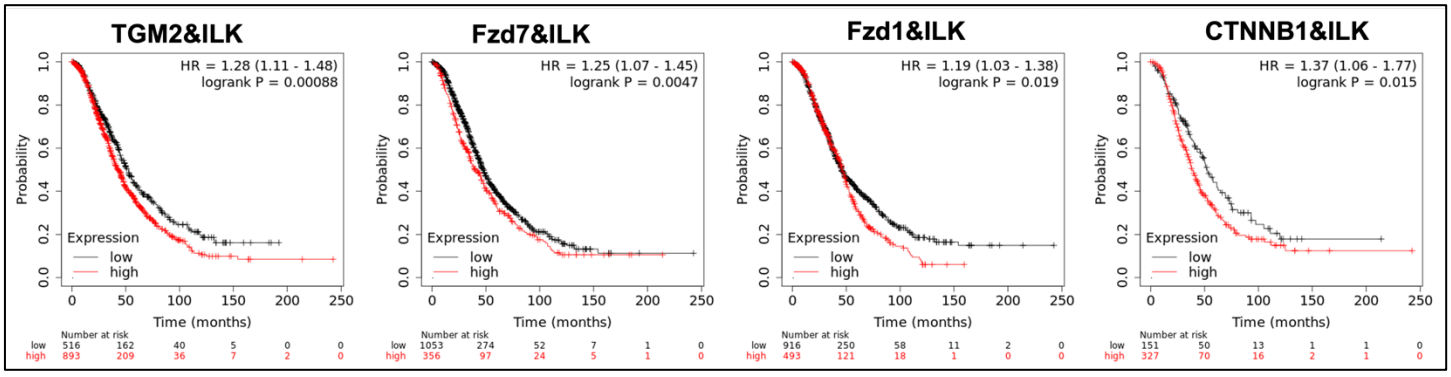

Figure 15: TG2 expression activates ILK in OC cells. Overall survival curves generated using the Kaplan–Meier plotter for tumors expressing high levels of TG2, Fzd7, Fzd1, and CTNNB1 in correlation with ILK versus those expressing low levels in HGSOC tumor microarray in patients treated with platin (TG2/ILK, P = 0.02; Fzd7/ILK, P=0.0047; Fzd1/ILK, P=0.019; CTNNB1/ILK, P=0.015).

What opportunities for training and professional development has the project provided?

Dr. Salvatore Condello, PI, received training for LARC (Laboratory Animal Resource Center) Basic and Advanced Mouse Manipulation, LARC Rodent Anesthetic Equipment Training, tissue specimens processing for Immunohistochemistry, tissue slides staining for immunohistochemistry.

Dr. Prasad Mayuri, Postdoctoral Fellow received training in ovarian cancer stem cells, Flow Cytometry analysis, FACS-sorting for markers associated with the phenotype, isolation, characterization, and culture of primary cells from OC ascites, Extreme Limiting Dilution software application for extreme limiting dilution analysis (ELDA), transduction and transfection of ovarian cancer cells, use of recombinant proteins, cell biology and animal studies, tissue specimens processing for Immunohistochemistry, tissue slides staining for immunohistochemistry.

Professional development activities included attending and presenting data at Annual DOD OCA Meeting, Monthly DOD OCA webinars, one-on-one DOD OCA Communication Coaching Sessions, monthly IUSCCC Seminar and Grand Rounds Series, monthly IUSM Department of Obstetrics and Gynecology Research Seminar Updates, weekly IUSM Department of Obstetrics and Gynecology Grand Rounds.

How were the results disseminated to communities of interest?

Results were disseminated by presenting data at the Virtual retreat of IUSCC-Tumor Microenvironment and Metastasis (TMM) research program, October 2020; Research Group Meeting in the Department of Obstetrics and Gynecology, IUSCC. March 2021; Monthly DOD OCA webinars on June 202.

What do you plan to do during the next reporting period to accomplish the goals?

To complete the Major Task 1 goals we continue collecting, processing, and staining for IHC tumor biopsies, human fallopian tube epithelium samples, and organoids from PDX.

In collaboration with the IUSM Pathology Core and the IUSM Tissue Procurement and Distribution Core we collected 96 human specimens in pair frozen and embedded in paraffin: 10 normal fallopian tube, 10 normal adjacent fallopian tube, 13 paired primary tumors and metastasis, 11 OC primary tumors, 30 metastasis, 12 normal adjacent-OC primary tumor pairs, 10 normal adjacent-OC primary tumor-metastasis paired. The specimens have been used to prepare TMA slides and for protein-RNA extraction. One of the slides has been used for the CD166 staining in Fig. 3A, more slides have been used for the proposed mIHC and for the PLA experiments described in Project 2 (Fig. 10E).

We are still working on building a homology model for the human CD166, Fzd1 and LRP6 to define novel PPI with TG2. We are performing co-IP analysis with recombinant TG2 wild type and mutants and CD166, Fzd1 and LRP6 are. Studies exploring co-localization of His-tagged TG2 mutant constructs with Fzd1, Fzd7, and LRP6 in OC cell lines are ongoing. Next, we will measure β-catenin activation by reporter activation, β-catenin and target genes (c-Myc and cyclin D1) expression levels will be measured in basal state and after Wnt ligands (Wnt3a/7a) treatment. Beta-catenin cellular distribution (nuclear vs. cytoplasmic) will be analyzed by confocal microscopy. We already performed some of the proposed experiments detecting β-catenin activation and

target genes expression during the Project 2 (Figs. 11C and 12G-J). We are planning to continue working in the near term to correlate β-catenin activation with chemoresistance.

4. Impact

What was the impact on the development of the principal discipline(s) of the project?

Ovarian cancer OC is the deadliest gynecological malignancy and its aggressive manifestations impact dramatically the life of patients. Despite enormous progresses in cytoreductive surgery and platinum-taxane based chemotherapy, the 5-year-overall survival remains low, mainly due to peritoneal recurrence. This has been attributed partly to persistence of ovarian cancer stem cells (OCSCs) at the end of primary treatment. The plasticity of OCSC allows them to survive and to be enriched during disease progression as well as after chemotherapy. Therefore, development of novel therapeutic strategies exploiting key biological mechanisms regulating cancer progression will significantly impact outcomes of patients suffering the complications of this aggressive cancer.

The focus of our research is to understand how TG2, an enzyme found to be active in ovarian tumors, protects OC and OCSC and stimulates their growth. We found that TG2 is enriched at the membrane of OCSCs forming a complex with several receptors, such as integrins, which allow the OCSCs to attach and grow in the peritoneal space. We provided evidence that tissue transglutaminase binds to the cellular receptors of the oncogenic Wnt pathway Frizzled1, 7 and co-receptor LRP6. This interaction stimulates survival pathways and stemness-related genes expression promoting OCSC. Our studies during the funded period provided several important implications. First, we defined the key amino acids sequences promoting tissue transglutaminase interaction with the Wnt receptor Fzd7. This discovery will allow us to synthesize a specific peptide directed against the amino acid residues responsible for tissue transglutaminase-Frizzled 7 interactions. The newly synthesized peptide will then be used to develop a specific monoclonal antibody that could specifically disrupt the complex between tissue transglutaminase and Frizzled 7 and eliminate cancer residual after chemotherapy. Second, we discovered the Wnt receptor Frizzled 1 and co-receptor LRP6 as potential interacting partners for TG2. Studies are ongoing aimed at defining the biochemical mechanism of this interaction. Third, we discovered the CSC marker CD166 as novel tissue transglutaminase-Frizzled 7 regulated gene. This mesenchymal stem cell marker is one of the adhesion molecules involved in several steps of the metastatic progression and its modulation impacts the crosstalk between cell-cell and cell-matrix adhesion leading to impaired ability of melanoma and colorectal to metastasize. CD166 expression has never been investigated in OCSC. Recently, we identified a new functional link between the TG2 regulated cell adhesion to the matrix, integrin linked kinase (ILK) phosphorylation and canonical Wnt signaling activation, proposing ILK as a central node of two combinatorial signals. Our findings indicate and provides important insights regarding ILK as possible therapeutic target in pre-clinical ovarian cancer models.

Our preliminary studies have the potential to introduce a novel paradigm linking the TG2-Fzds-mediated Wnt pathway activation as important regulator of OC progression and the OCSC phenotype.

What was the impact on other disciplines?

Cancer stem cells (CSC) which possess self-renewal properties and genomic instability are considered to be a hallmark of all solid tumors. A better understanding of the key regulators involved in ovarian cancer stem cell (OCSC) survival is needed and developing strategies to target these chemo-resistant cells has the potential to have a significant and sustained impact on treatment resistance in other solid tumors. In the longer term, we believe delivering a novel approach for targeting ovarian cancer stem cells that can eliminate cancer cells surviving after standard chemotherapy that could be used for other cancers as well. As TG2 and Fzd7 are frequently deregulated in other cancers, the impact of this on other disciplines would include the development of antibody specific therapy based in combination with current platinum-based therapy as a novel treatment to inhibit expansion of resistant cancer cells.

What was the impact on technology transfer? Nothing to report

What was the impact on society beyond science and technology?

The development of novel strategies targeting CSCs is highly relevant, as these cells are responsible for tumor recurrence after chemotherapy and the fatality of ovarian and other cancers. Our study will provide new results to help understanding the key regulators of tumor recurrence proposing new therapeutic target to the forefront for patients diagnosed with early and advanced disease. The long-term goal is to provide a new potential therapeutic target to block tumor progression, enhancing the quality of life and welfare after cancer treatment for women and their families.

5. Changes/Problems

Changes in approach and reasons for change. Nothing to report

Actual or anticipated problems or delays and actions or plans to resolve them:
One of the major challenges encountered during the funded period was still correlated with COVID-19 pandemic. We experienced difficulties in obtaining tumor biopsies for tissue slides preparation. As a consequence, the Major Task 1-Subtask 4 and 5 are experienced a delay in the proposed SOW.
In collaboration with the IUSM Pathology Core and the IUSM Tissue Procurement and Distribution Core we collected 96 human specimens in pair frozen and embedded in paraffin, as described above. The samples have been already processed (embedded and sectioned) and are currently used for the multiplex IHC (mIHC) and proximity ligation assay (PLA) analysis to map the TG2 expression in correlation with Wnt ligands, Wnt receptors, downstream signaling and target molecules in heterogenous tumor cell populations. Some results have been already obtained and included in the Projects 1 and 2. Other studies are ongoing. In addition, primary OC cells grown as organoids from eight patient's ascites have been already processed and will be used for the proposed mIHC and PLA analysis.

Changes that had a significant impact on expenditures. Nothing to report

Significant changes in use or care of human subjects, vertebrate animals, biohazards, and/or select agents. Nothing to report

Significant changes in use or care of human subjects. Nothing to report

Significant changes in use or care of vertebrate animals. Nothing to report

Significant changes in use of biohazards and/or select agents. Nothing to report

6. Products

Publications, conference papers, and presentations.

1. Ovarian Cancer Academy Webinar Work in Progress discussion.
   Salvatore Condello, PhD.
   Presentation Title: "CD166 as novel therapeutic target to overcome platinum resistance in ovarian cancer". Jun 8, 2021.

2. Research Group Meeting.
   Salvatore Condello, PhD.
   Presentation Title: "Targeting Ovarian Cancer Stem Cells Interactions with the Tumor Niche".
   Department of Obstetrics and Gynecology, IUSCC. March 29, 2021.

3. IUSCC-Tumor Microenvironment and Metastasis (TMM) research program.
   Salvatore Condello, Ph.D.
   Presentation Title: "Tissue transglutaminase as a key regulator of Ovarian Cancer Stem Cells Interactions with the Tumor Niche". Virtual retreat. October 1, 2020.

Journal publications. Nothing to report

Books or other non-periodical, one-time publications. Nothing to report

Other publications, conference papers, and presentations. Nothing to report

Website(s) or other Internet site(s). Nothing to report

Technologies or techniques. Nothing to report

Inventions, patent applications, and/or licenses. Nothing to report

Other Products. Nothing to report

7. Participants & Other Collaborating Organizations

Name: Salvatore Condello, PhD
Project Role: PI
Nearest Person month: 12
Contributions to Project: Dr. Condello performed work on the culture of cells, cell sorting, molecular biology, cell transfection/transduction, primary cell isolation, tissue specimen processing for IHC, immunofluorescence, PLA, manuscript writing.

Name: Mayuri Prasad, PhD
Project Role: Postdoctoral Fellow
Nearest Person month: 12
Contributions to Project: Dr. Prasad performed work on the culture of cells, cell treatments, cell sorting, molecular biology, cell transfection/transduction, primary cell isolation, tissue specimen processing for IHC, PLA, immunofluorescence, animal work, manuscript writing.
Funding Support: Award W81XWH1910008 and 10% on start-up funding, matching the NIH Salary Cap.

8. Special Reporting Requirements. Nothing to report

9. Appendices. Nothing to report